Probes of top compositeness at the Large Hadron Collider

Romain Kukla

Master of Science thesis
Performed at CEA Saclay and CERN

Supervisor : Jonas Strandberg
Local supervisor CEA : Anne-Isabelle Etienvre
Local supervisor CERN : Géraldine Servant

TRITA-FYS 2014 :10
ISSN 0280-316X
ISRN KTH/FYS/–14 :10—SE

Particle and Astroparticle Physics
Department of Physics, School of Engineering Science
KTH Royal Institute of Technology, SE-106 91 Stockholm, Sweden
August 2013

Abstract

After the Higgs boson hunt, the LHC could be a powerful tool to unravel the mystery of which exotic physics lies beyond the realm of the Standard Model. Different new physics sectors have been postulated, among them the supersymmetric one has gained a very popular interest. There are still other compelling alternatives to SUSY such as composite models which we are dealing with. We focus on the top compositeness scenario as an extension of the SM, in two ways : first, considering a top-philic heavy Z' boson which couples only to the top and secondly, studying the $T_{5/3}$ exotic top partner emerging from the composite sector. Both have a very specific signature, $t\bar{t}t\bar{t}$ or similarly $t\bar{t}WW$ final states, motivating a same-sign dilepton analysis. One needs to wait $\sqrt{s}$ =14 TeV to have a significant number of events for the Z' but as for now the 8 TeV data analysis can still give useful constraints on the $T_{5/3}$ mass.

Keywords

Exotic physics, Standard Model (SM), Beyond the Standard Model (BSM), Electroweak symmetry breaking (EWSB), Top exotic partners, $T_{5/3}$, Z', compositeness, same-sign dilepton analysis.

Contents

Contents **4**

Introduction **6**

1. The LHC and ATLAS **9**
1.1 The machines 9
1.2. Data acquisition and processing 12
1.3. Objects reconstruction 13
1.4. Simulation tools 15

2. Composite Models in BSM **17**
2.1. The Standard Model and its defects 17
2.2. Top-philic Z' boson 20
2.3. Top exotics partners 21
2.4. Same-sign dilepton channel 24

3. Z' discovery potential of the same-sign dilepton channel **25**
3.1. Samples and methodology 25
3.2. Cuts 29
3.3. Extensions 30

4. Z' discovery potential of the trilepton channel **33**
4.1. Motivation 33
4.2. Cuts 35

5. $T_{5/3}$ SS dilepton analysis **39**
5.1. Outline and motivation 39
5.2. Cuts in TopRootCore 42

Conclusions and Outlook **45**

List of figures **47**

References **48**

Aknowledgments **50**

Introduction

Though the composite nature of matter and the concept of a continuum were postulated by philosophers very early in History, physics had to wait until the 19^{th} century to start considering atoms exist and elaborate subatomic theories. In a sense, particle physics was born in 1897 when Thomson observed the electron - the first elementary particle to be discovered !

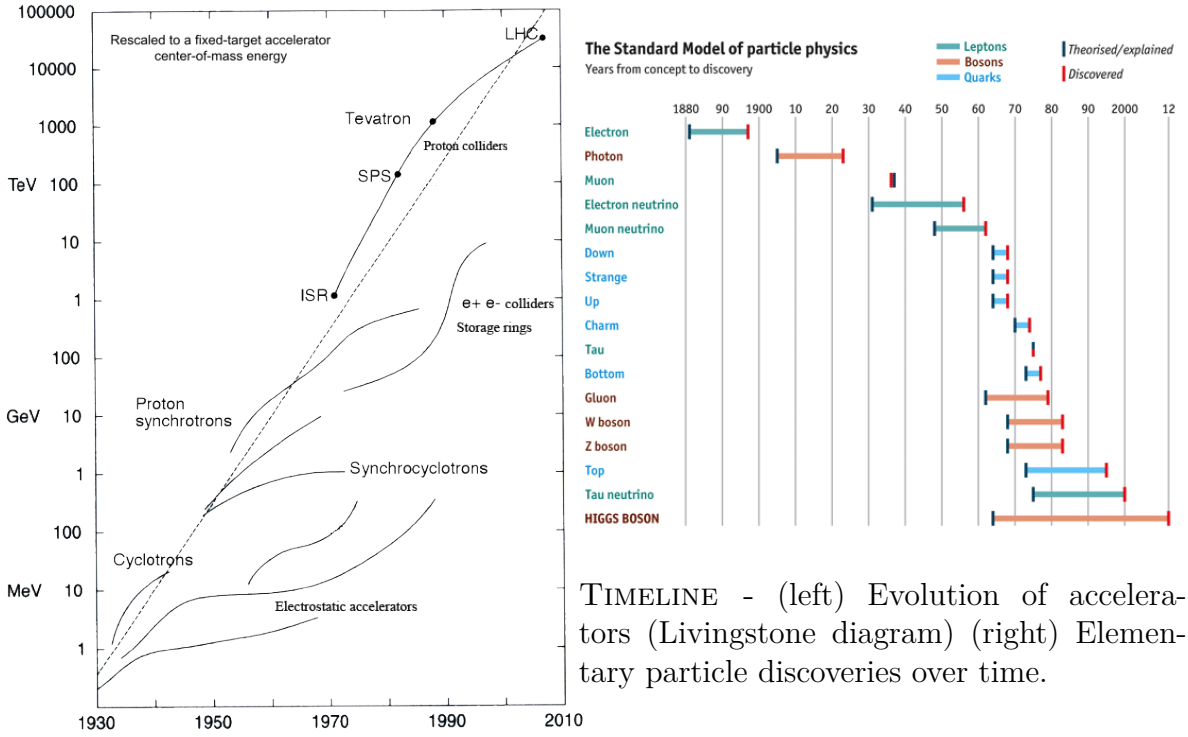

Timeline - (left) Evolution of accelerators (Livingstone diagram) (right) Elementary particle discoveries over time.

After the quantum revolution, nuclear research opened the way towards more and more powerful accelerators. The particle zoo was increasing each year, as was the theoretical understanding of what was about to become the Standard Model (SM). Meanwhile, the field underwent a profound change in the structure of research with the emergence of international collaborations, which is in an historical perspective another grand success for mankind. As for now, CERN is the leading research facility in hadronic physics in the world, mainly focused on SM completion and extension. The two dedicated collaborations, ATLAS [1] and CMS [2], are a very prolific community, analysing every piece of data to constrain every model measuring masses, widths and other physical properties. Impressively, the current status is that the SM is consistent with every measurement done, as seen in figure 1 [3, 5].

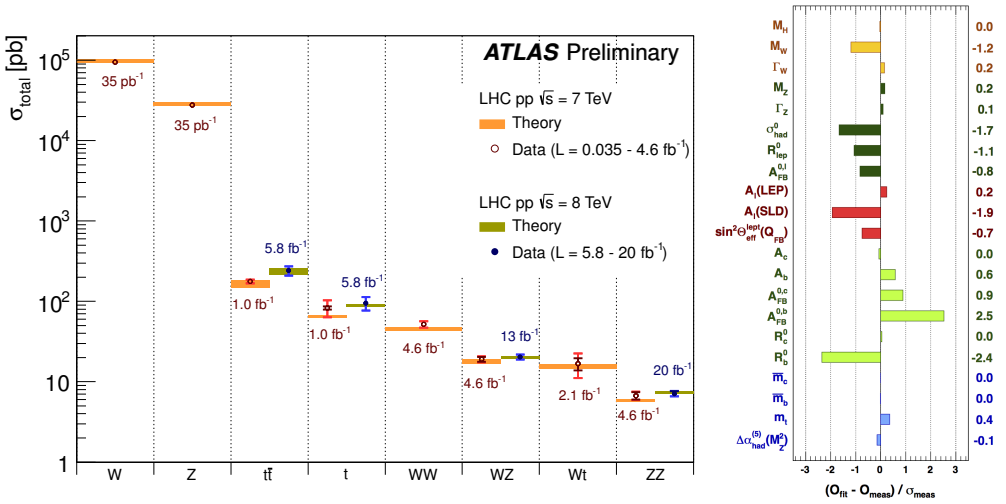

FIGURE 1 – (left) Main SM production cross-sections at LHC with 2011 and 2012 data (right) Precision measurements of SM parameters with 2011 data

After the events of July, 4^{th} 2012, Moriond 2013 conference and the resulting Nobel Prize, the SM is complete with the last piece being the Higgs boson [6]. One question remains open : as we have seen no real discrepancy in the precision measurements with 21.7 fb^{-1} of 8 TeV data, will the LHC see something more after the shutdown ? The supersymmety, which postulates the existence of a superpartner for each particle, has been searched for years (fig. 2).

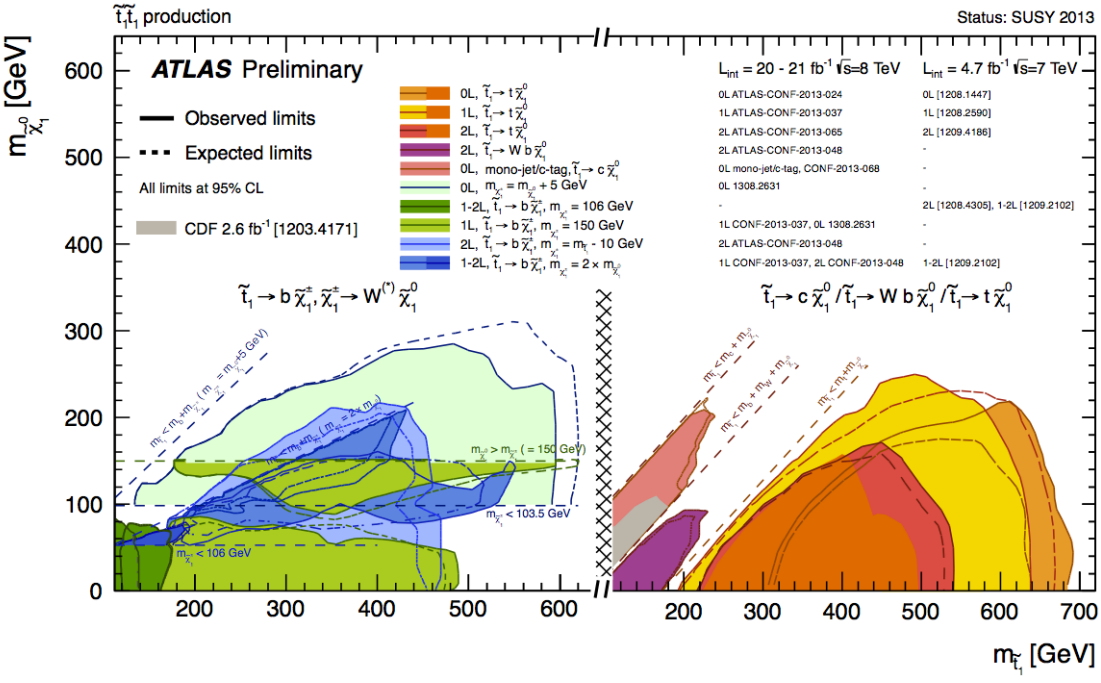

FIGURE 2 – Summary of ATLAS constraints on direct stop production for different decay modes using 21 fb^{-1} at $\sqrt{s}$=8 TeV

BSM physics, which tries to extend the SM and address its drawbacks, does

not reduce to SUSY : other models exists, forming the exotic physics. But the limits put on exotics models [5] (see fig. 3) tend to reach high masses compared to SM particles, which could be worrying for the future of collider physics.

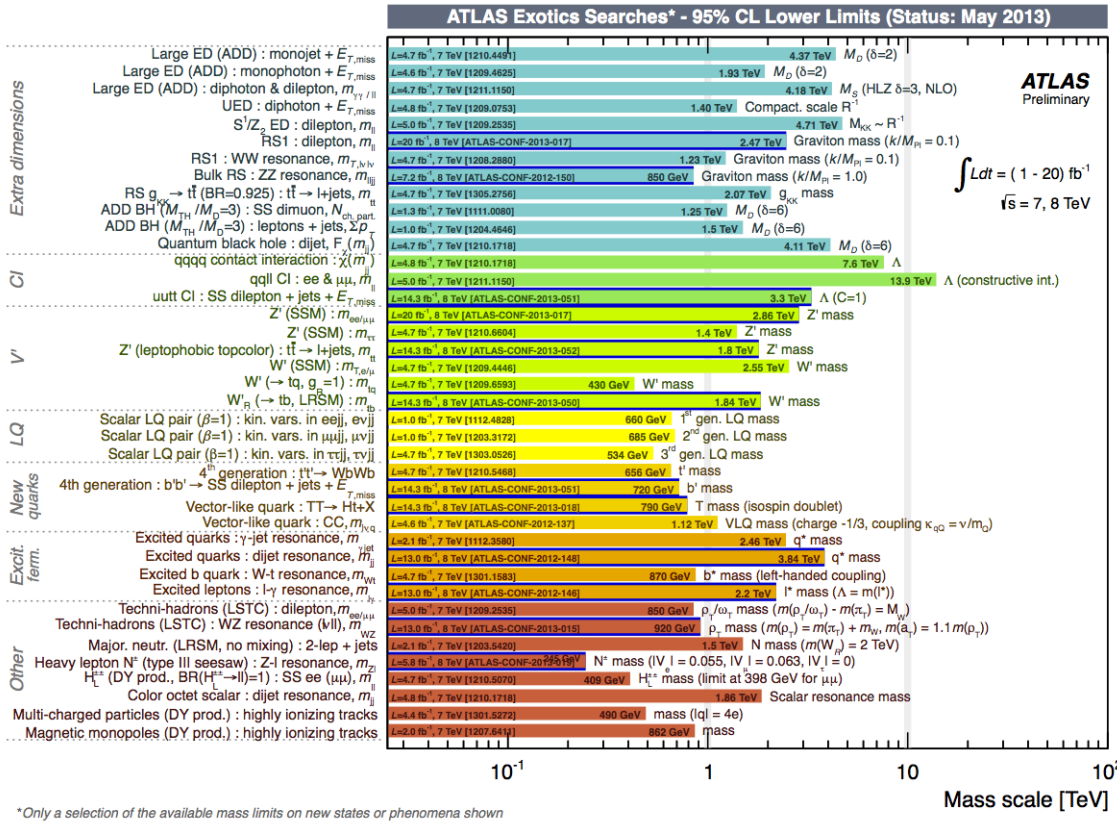

FIGURE 3 – Combination of ATLAS mass limits for exotics studies (full data)

This master thesis consists in exploring an exotic set of SM extensions, namely the composite models, which could be a strong alternative to SUSY. I had the great opportunity to work on two different approaches of these models : a phenomenological one with G. Servant at CERN PH-TH, on a generic top-philic model which can be easily adapted to any composite model ; and an experimental one with A-I Etienvre at CEA Saclay in the ATLAS team on a specific top exotic partner. Their former PhD student Léa Gauthier has already worked on this, so I took over and present here my update of her studies.

Chapter 1 is a global overview of the technical and scientific context. I present very briefly the LHC, the ATLAS detector. Then, the objects I will use in my analysis, what they represent and how they are produced.

Chapter 2 is a theoretical description of the models and new particles I will study, the heavy Z' and the $T_{5/3}$. I also present the appropriate channel.

Chapters 3 and 4 describe the phenomenological study of the Z'(1 TeV) at $\sqrt{s}$=14 TeV, respectively with the dilepton channel and the trilepton channel.

Chapter 5 is the $T_{5/3}$ dilepton analysis at $\sqrt{s}$=8 TeV with 21.7 fb^{-1} data. I present the different steps of this study which is still in progress.

1. The LHC and ATLAS

1.1 The machines

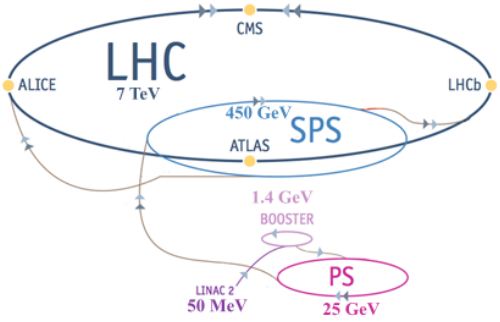

FIGURE 4 – LHC at CERN

The *Large Hadron Collider* (LHC), the most powerful proton-proton collider in the world, located at CERN, was designed to have a nominal center of mass energy of $\sqrt{s}$=14 TeV, 7 TeV for each proton. It consists in a succession of accelerating and storage rings which inject two proton beams in opposite side in a 27 km long collider. It replaces the LEP, which was an e^+e^- collider in operation until 2000. The LHC took over the Tevatron, at Fermilab, a $p\bar{p}$ collider which ran with a nominal energy of 1.96 TeV. When its shutdown occurred in 2011, the Higgs boson mass range was constrained by the LEP and the Tevatron exclusion limits (between 115 and 140 GeV, or over 180 GeV) [7].

The LHC experiments consist in four detectors and their collaboration :

- ALICE [8] studies heavy ion collisions and *quark-gluon plasma* using Pb nuclei at $\sqrt{s}$=2.76 TeV for each nucleon pair.
- LHCb [9] focuses on CP violation linked to the b quark. More generally, it tries to observe very rare decays of B mesons.
- CMS and ATLAS [2, 1] are dedicated to the search of the Higgs boson but also test the SM and find any BSM.

With a bunch spacing of 50 ns, about 20 million of bunch crossings occur each second at each collision point. First, the LHC ran with a c.o.m energy of 900 GeV, then 7 TeV (2009-2011) and ultimately 8 TeV in 2012. The resulting luminosity registered by ATLAS is shown in fig. 5. During the current long-shut down, every magnet will be checked and the detectors will be upgraded so that in 2014, the LHC will reach 13 TeV and then hopefully the nominal energy. After the second upgrade, the instantaneous luminosity is expected to be ten times bigger. The integrated luminosity $\mathcal{L}$ is a critical parameter because it is correlated to the number of collisions ($N = \mathcal{L}\sigma$).

Table 1 shows some processes with their cross-section at different energies. One can see that the $t\bar{t}$ pair production is very dominant, indeed the LHC is said to be a "top factory". For many studies involving top quarks, $t\bar{t}$ constitutes the main background.

Process	$\sqrt{s}$ (TeV)	σ
pp $\rightarrow t\bar{t}$	14	442 pb
pp $\rightarrow t\bar{t}$	7	93 pb
pp $\rightarrow t\bar{t}t\bar{t}$	14	7.5 fb
pp $\rightarrow t\bar{t}t\bar{t}$	7	0.74 fb

TABLE 1 – Cross-sections for $t\bar{t}$ and $t\bar{t}t\bar{t}$ at $\sqrt{s}$ =7 and 14 TeV

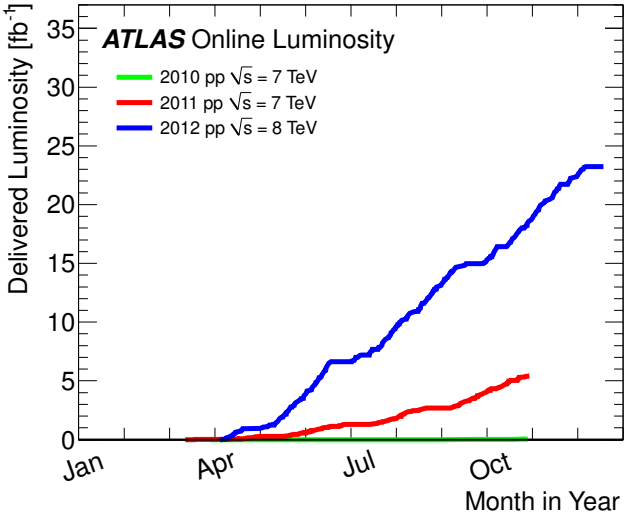

FIGURE 5 – ATLAS luminosity

Instinctively, we could think that we should increase the energy endlessly to observe even rare processes, but we are limited by the magnet technology. Also other technical limitations arise such as the *pile-up* effect, which is the number of interactions in the same collision inside the detector.

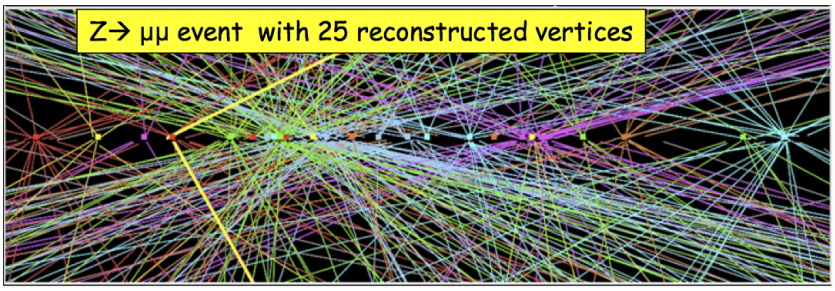

FIGURE 6 – Illustration of the pile-up effect

The pile-up is a real challenge as the software has to reconstruct each track and vertex to isolate valuable events, with some uncertainties. The higher the instantaneous luminosity gets the more pile-up we observe, as we see in fig. 7.

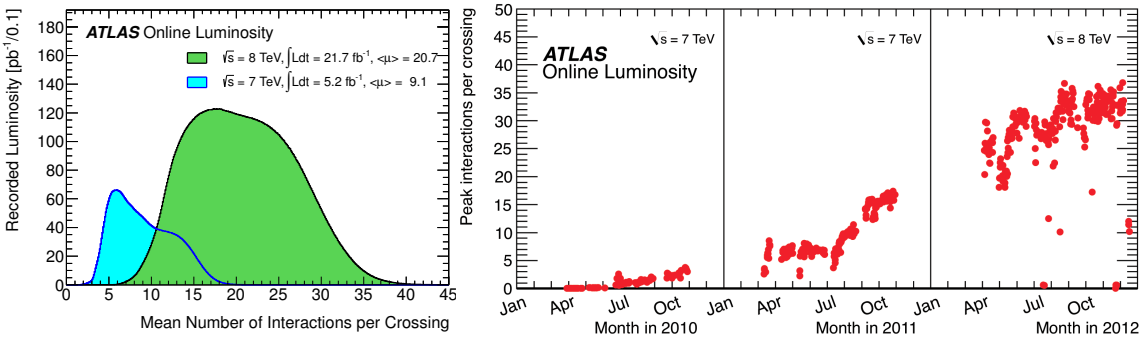

FIGURE 7 – (left) Pile-up spread for different instantaneous luminosities and (right) Pile-up evolution with time

A quick overlook on ATLAS reveals the enormous amount of embedded detectors which need to be wired, powered and monitored. With hundred thousands of data for each collision, without a powerful reconstruction algorithm which maps every energy deposit, electrical intensity and so on, to physical objects, the detector would be unreadable and useless.

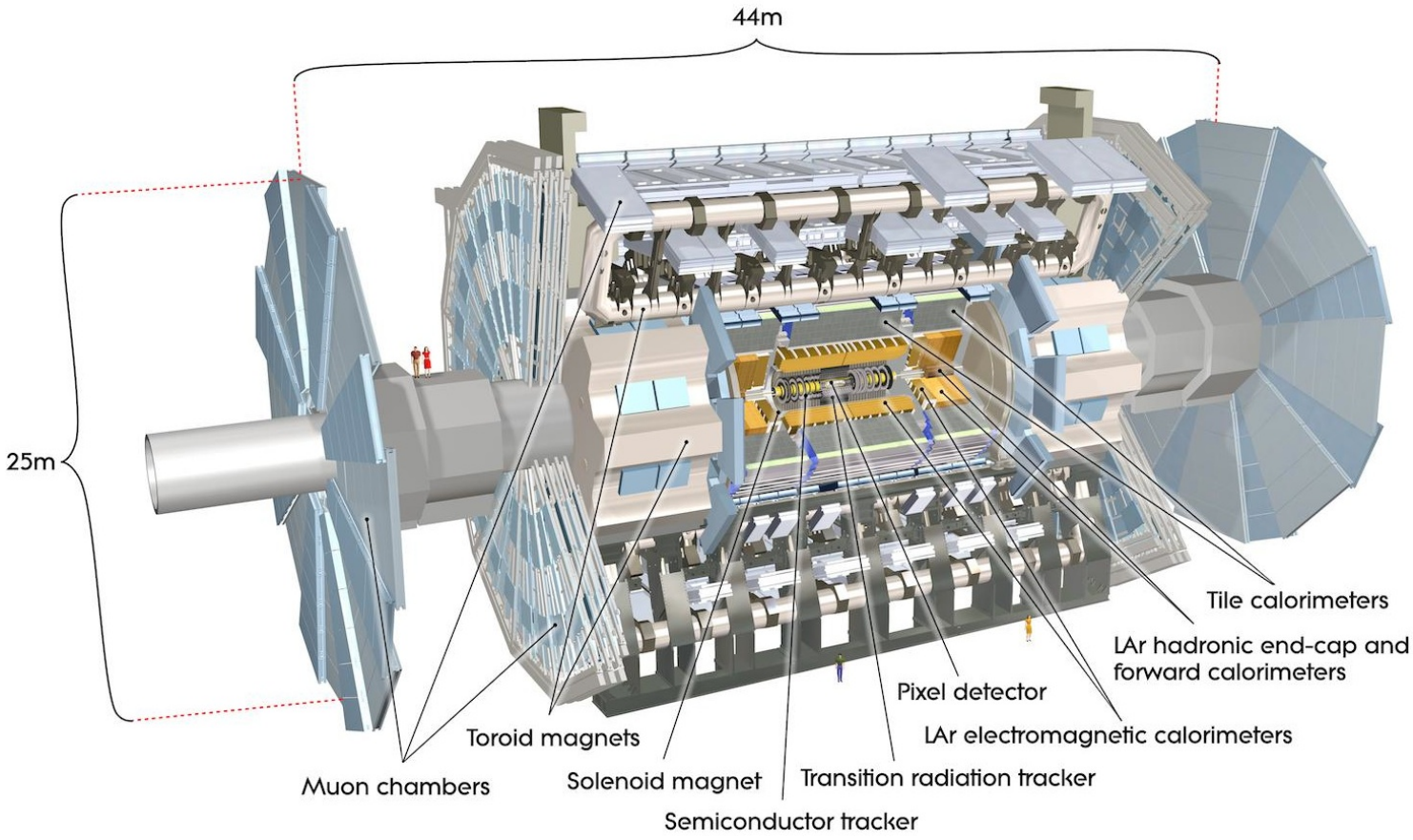

FIGURE 8 – Inner structure of the ATLAS detector

Without detailing every subarea, here are the main parts of the detector :

— the *inner detector* is a tracking device only for charged particles. The surrounding magnetic field curves the trajectory which is measured and thus gives the particle's charge and momentum.

— the electromagnetic and hadronic *calorimeters* absorb the energy of the incoming particles. The first one focuses on EM showers while the second one takes the hadronic showers.

— the *muon spectrometer* tracks the outgoing muons and measure their trajectory, which is bended by a magnetic field created by the toroidal magnets, giving again both charge and momentum.

ATLAS uses a cylindrical coordinate system, ϕ and θ defined such as : x axis points toward the center of LHC, y upwards and z being the beam axis. Thus, we have two relations using the pseudorapidity η (η points toward the particle scattering direction, η=0 being the transverse plane).

$$\phi = \arctan(\frac{x}{y}) \quad \text{and} \quad \eta = -\ln\tan(\frac{\theta}{2})$$

1.2. Data acquisition and processing

In order to keep only the interesting events, ATLAS has a trigger system which reduces the interaction rate from 1 GHz to 100 Hz. The first trigger level is directly implemented on the hardware watching the calorimeters and muons chambers activity, while the second trigger level is a software process which eventually sends the selected events to Tier-0 for reconstruction before being dispatched over the Grid (fig. 9).

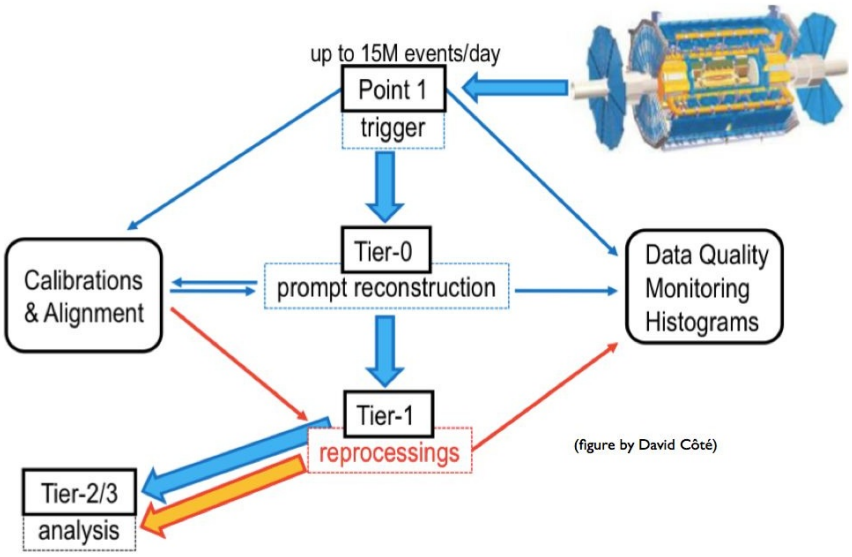

FIGURE 9 – Data processing path in ATLAS

The output of the trigger system is saved in different streams which are not exclusive. Tier-0 reconstructs from the streams different ROOT ntuple formats storing all the physical data and plenty of trigger informations. As the $T_{5/3}$ search is both in Exotics and Top working groups, the dedicated framework is TopRootCore, an analysis package using ROOT for such ntuples. Physics observables such as energy, momentum, pseudorapidity, ϕ, θ, missing energy, H_T, errors infos are stored in ROOT trees, a very powerful structure allowing to store and read thousands of events efficiently.

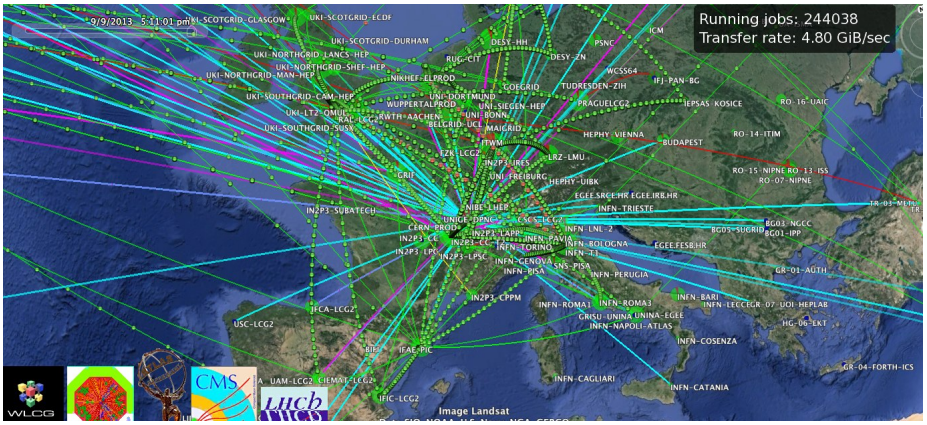

FIGURE 10 – Example of the grid traffic

Working with ATLAS data requires to use different frameworks. Storing huge datasets and processing them takes time and ressources for a tiny computing farm : to solve this, CERN has designed the worldwide LHC Grid which connects all HEP physicists to LHC data. It is divided into "tiers" : Tier-0 is CERN computer center, first read-out of the detectors' data and event reconstruction ; Tier-1 is a group of clusters (CCIN2P3 in France ; NDGF for Nordic countries) which stores the reconstructed data and dispatches them to Tier-2 national groups (GRIF for Paris ; SNIC for Sweden), mainly institutes, where only specific reduced datasets are locally stored for current analyses.

1.3. Objects reconstruction

With all this apparatus, the algorithm has to deduce from the calorimeters activity and the tracking devices which particle flew through the detector.

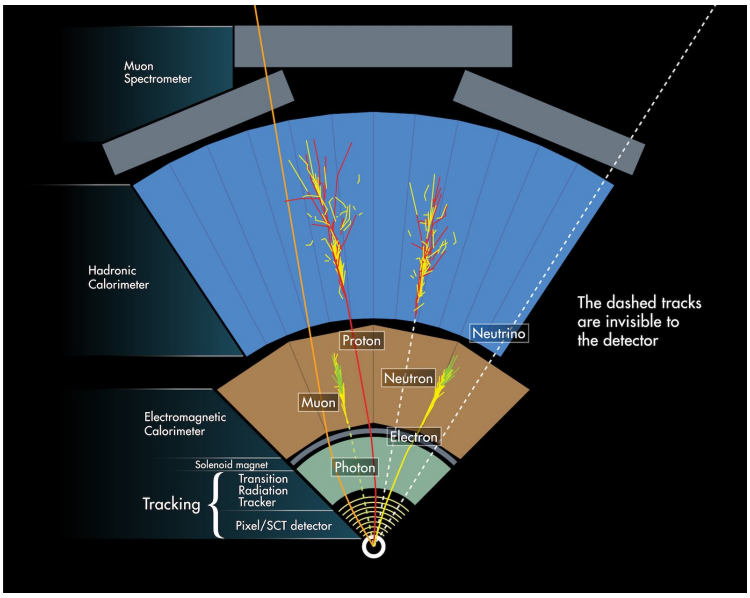

FIGURE 11 – Particle recognition pattern in ATLAS

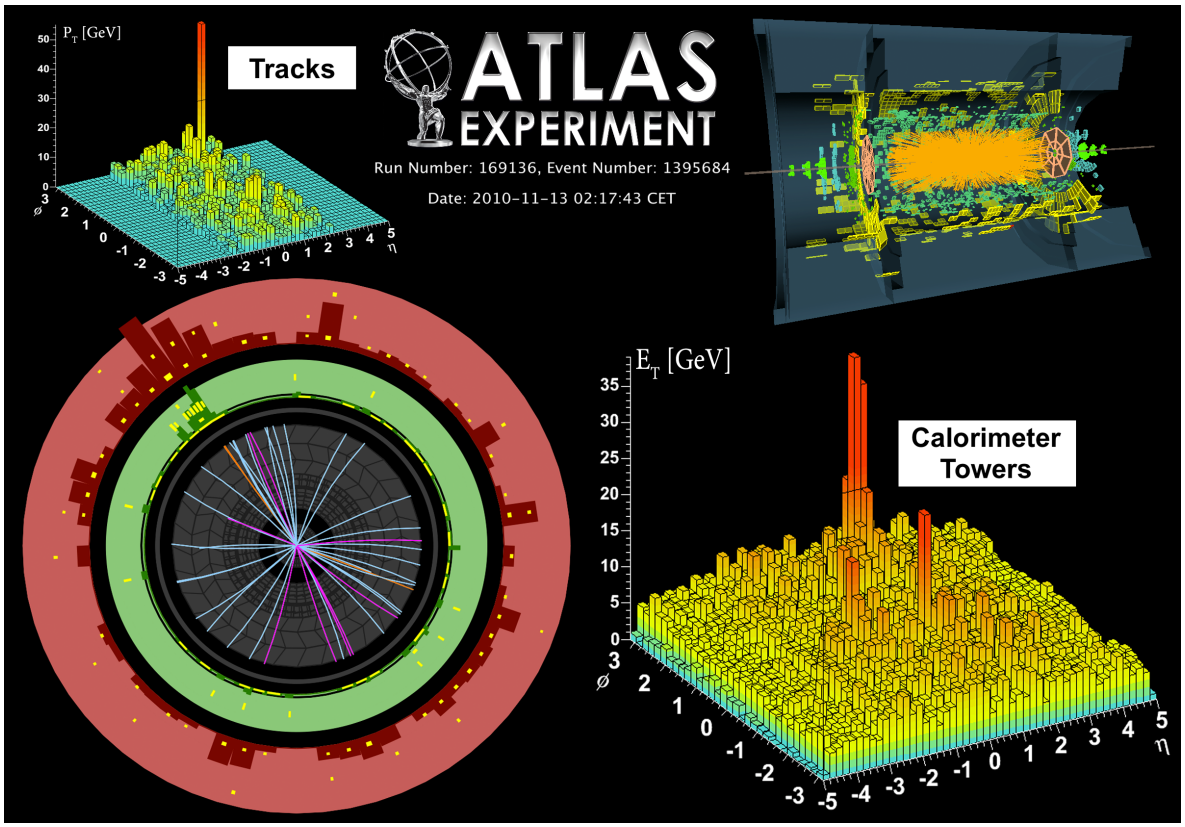

FIGURE 12 – Event display including calorimeter and tracking activities

In order to reconstruct the different particles, one needs to combine the different sub-parts of the detectors, such as the inner tracking device and the calorimeters. For instance, a particle would be said to be an electron if there is a track in the inner detector and an energy cluster in the calorimeter (fig. 11). The algorithm extrapolates the direction of the electron in the inner tracker to the EM calorimeter before forming the optimal cluster using energy deposit (fig. 12). For the muons, one searches for a track and a signal in the muons spectrometer, extrapolating the first one from the last one in some cases. Both for electrons and leptons, there are different reconstruction strategies which gives multiple categories of reconstructed leptons. Depending on the analysis, physicists will choose which one to use.

For the jet reconstruction, some topological clusters are formed in the calorimeter where the energy deposit is above the background and then one of the two leading algorithms used by ATLAS is chosen : the cone or the anti-k_T algorithms [10, 11] :

— **The cone algorithm** is parametrized by the cone's radius R (typically 0.4 or 0.6). The program starts to seed initial cones from high energy density regions and overlap them with particles until a stable cone is found. A stable cone is then a set of particles that are within a distance R in the $y - \phi$ plane around their center of mass.

— **Anti-k_T** is a sequential algorithm. It first defines initial protojets like before, then calculates a weight including p_T and protojets relative distance, takes the minimal value and then either reconstructs a jet either combines two protojets and loops. "Anti" in the name refers to an improvement of the k_T algorithm which clusters the protojets around the boosted hadrons and gives better results.

The neutrinos can be inferred by a high missing transverse momentum in the transverse plane, as $\sum |p_T| = 0$.

1.4. Simulation tools

To compare the observed data to what we should expect, we need to generate events directly from the theoretical description of the SM. This is done using Monte-Carlo generators which are probabilistic algorithms which choose random inputs from a probability distribution over the domain we study and compute the results for each determined input. They are used for calibrating algorithms or uncertainties in experimental analyses and for prospective studies in exotic phenomenology. MC generators perform large numbers of phase-space integrals and provide particle data for each event. Given an exotic lagrangian with its Feynman rules, everyone can implement a new model and generate processes and events.

There are three steps in MC :

— **Parton level** (*MadGraph*) events describe the process in terms of quarks, leptons and bosons only.
— **Hadronization** (*Pythia*) includes QCD : radiation in the initial and final states and forms the hadronic showers from quarks.
— **Detector level** (*PGS*) adds detector effects to compare MC data with experimental ones.

MadGraph output format (Les Houches events file), is a standard interface with other MC tools. MadGraph4 [12] is a LO MC generator, in fortran, but MadGraph5 [13], in C++, has replaced it as it is way more efficient.

2. Composite Models in BSM

I present here the main motivations for such models. The Z' model has been elaborated by G. Servant [17] and the $T_{5/3}$ model [15] is now getting more and more attention as a probe of top compositeness.

2.1. The Standard Model and its drawbacks

The discovery of a SM-like Higgs boson is not the end of the story. It confirms that the electroweak symmetry breaking (EWSB) as described as the Higgs mechanism is accurate, but one needs to measure every coupling to the Higgs boson to be sure that it is the SM scalar boson.

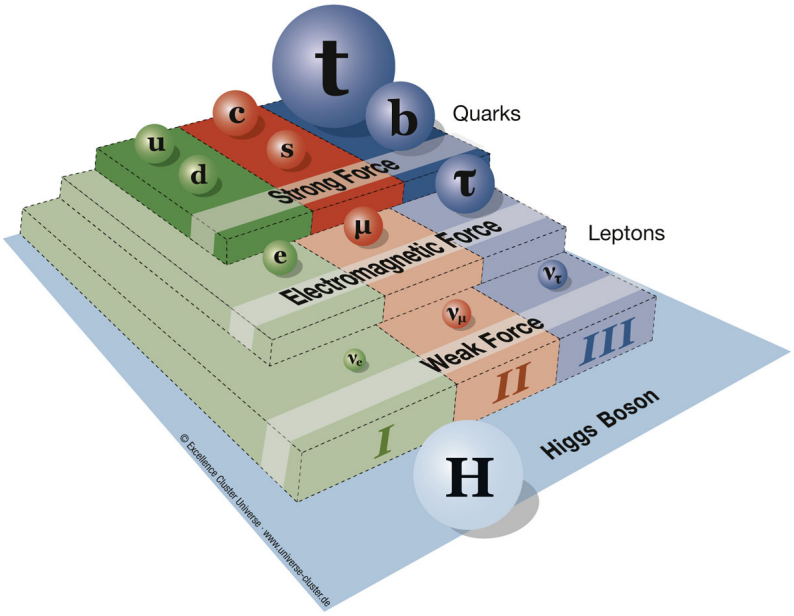

FIGURE 13 – Relative size of the masses of SM particles (not to scale)

The SM is a quantum field theory described by the gauge symmetry group $SU(3)_c \times SU(2)_L \times U(1)_Y$, where $SU(3)_c$ contains the QCD generators (gluons) and $SU(2)_L \times U(1)_Y$ unifies the electroweak force, initialy formed by QED $U(1)_Y$ (mediated by B) and the weak force (mediated by W_1, W_2 and W_3). As the charge is not invariant in the weak isospin space, the unificated EW force is generated by the 4 bosons, B, W_1, W_2 and W_3. They should be massless to ensure the symmetry group but we observe intermediate massive bosons. The Higgs field, as a $SU(2)$ doublet, breaks the EW symmetry giving rise to three Goldstone bosons and the Higgs. The three emerging bosons, being coupled to EW bosons, mixe and create the massive intermediate bosons, the photon staying massless as the generator of the unbroken EW gauge group (see fig.14).

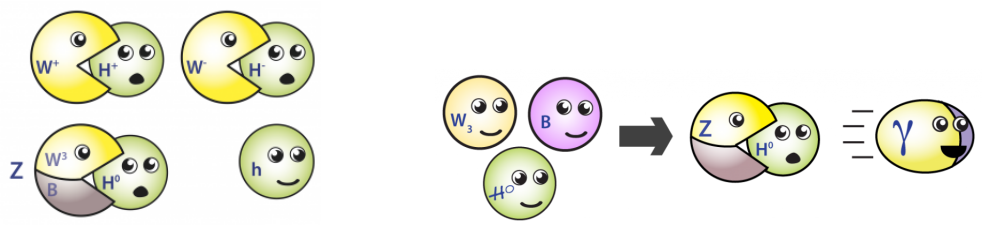

FIGURE 14 – EWSB sketched by Flip Tanedo on `www.quantumdiaries.org`

This mathematical formalism based on Lie algebra and symmetry groups [21] structures the SM in three categories : the matter (quarks, leptons), the interactions (gauge bosons) and the Higgs boson as seen in fig.15 [20]. To each particle corresponds an antiparticle with same mass but opposite charge.

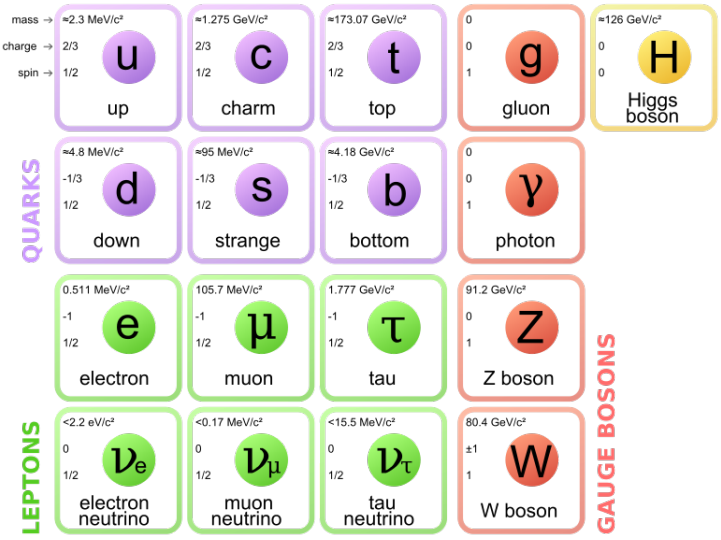

FIGURE 15 – The Standard Model of particle physics in 2013

The matter consists in elementary fermions which are organised in 3 families, or generations, sorted in increasing mass. They are divided in two groups :

Leptons	**Quarks**
$\begin{pmatrix} e \\ \nu_e \end{pmatrix}$ $\begin{pmatrix} \mu \\ \nu_\mu \end{pmatrix}$ $\begin{pmatrix} \tau \\ \nu_\tau \end{pmatrix}$	$\begin{pmatrix} u \\ d \end{pmatrix}$ $\begin{pmatrix} c \\ s \end{pmatrix}$ $\begin{pmatrix} t \\ b \end{pmatrix}$
Do not interact via the strong force	Exist in 3 colors (QCD color charge)

The underlying mechanism is that the 3^{rd} generation decays to the 2^{nd} one and eventually to the first one. Thus, the usual matter is only made of up and down quarks and electrons ; the other particles are created in stars or colliders. Each fermion exists in two chirality states corresponding to the two components of the associated Dirac spinor which verifies the free lagrangian

$$\mathcal{L} = \bar{\Psi}(i\partial\!\!\!/ - m)\Psi$$

with $\Psi = \begin{pmatrix} \psi_L \\ \psi_R \end{pmatrix}$ the Dirac spinor and m the fermion's mass.

The fundamental interactions unify every phenomenon which occurs at particle level and are described by a force carrier, the vector boson. If two particles interact together, they exchange virtual bosons so the strength and the range of a force depend on the mass of the force carrier. There are three interactions :

— the **electromagnetic force** (photons γ) concerns only charged particles, 100 times smaller than the strong force
— the **weak force** (W^+, W^- and Z bosons) acts on left-handed fermions and is the only one to change its flavour. It is responsible for β decays. 10^8 times smaller than the strong force
— the **strong force** (gluons g) involves only quarks. It forms hadrons, mesons and confines quarks into pairs. The nucleus cohesion is due to this interaction. Gluons carries a color charge and can couple to itself.

The SM does not include the gravitation (described by the graviton) because its strength is negligible (10^{38} times smaller than the strong force). SM extensions like supergravity try to mix quantum field theory and general relativity to have the 4 interactions but they have not been yet discovered experimentally.

But the SM has defects : it does not explain the *neutrino oscillations* and their small mass ; there is no candidate to *dark matter* ; the *matter-antimatter asymmetry* is not solved ; there are still *free parameters* which are not predicted ; the strong and electroweak forces do not seem to *unify* at high scale ; the *hierarchy problem* in the Higgs boson mass remains.

Compositeness main interest comes from theoretical connections between higher-dimensional gravity and strongly-coupled gauge theories (AdS/CFT correspondance) [31]. The composite Higgs boson would take place in the bulk of an extra dimension model such as Randall-Sundrum [23]. The idea is to postulate a strong sector beyond the TeV scale where composite states are strongly coupled. Such a strong sector is parametrized by a mass scale and a coupling constant. If we consider that the composite states are linearly coupled to the SM fermions, it means it should exist a basis in which the SM and composite particles are coupled only by a mass matrix mixing ; thus, the common SM fermions appear to be a mixing between elementary and composite states [24].

In composite models, the Higgs boson either does not exist either is a composite particle from the strong sector. This means that it appears to be a pseudo-Goldstone boson of a new symmetry breaking from the strong sector [14]. As the top quark mass and its corresponding Yukawa coupling to the Higgs boson are high, the composite sector would couples mostly with it instead of the first and second generation. In such case, the Higgs boson mass will be stabilized by the contribution of the new exotic top partners [15]. Dark matter candidate, such as a heavy neutrino, can be also added to these models [16].

2.2. Top-philic Z' boson

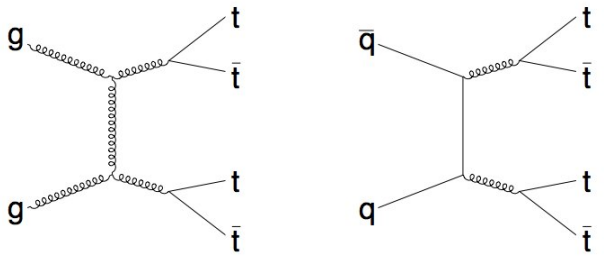

FIGURE 16 – SM four tops events

Four top quarks final states occur in SM from the diagrams in fig. 16 and are dominated by gluon fusion. The corresponding cross-section is about 7.5 fb at 14 TeV and can be enhanced to 30 fb with additional jets. Because of this small SM cross section, these events are very sensitive to BSM contributions. In particular, the cross section is enhanced in models of top compositeness (the so-called models of "top-philic" new physics"). One could consider any strong resonance such as in fig. 17, leading to 4 top quarks final states. The top-philic model is a generic model containing a new vector resonance which has a strong coupling to top quark. This is not stricto sensu a composite model but a tool to study 4-top events as would occur in BSM models of top compositeness.

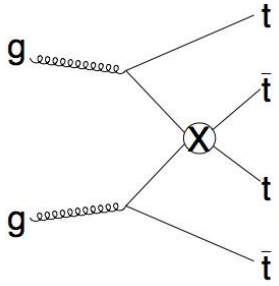

FIGURE 17 – Top-philic resonance in $t\bar{t}t\bar{t}$ states

Let us consider a new exotic resonance, a massive Z' boson, coupled only to the right-handed top, with a mass of 1 TeV [1], produced following fig. 18 diagrams.

FIGURE 18 – Resonant production diagrams for Z'

The SM lagrangian is extended to :

$$\mathcal{L} = \mathcal{L}_{\mathcal{SM}} - \frac{1}{4}F'_{\mu\nu}F'^{\mu\nu} + M^2_{Z'}Z'_\mu Z'^\mu + g^t_R \bar{t}\gamma^\mu P_R Z'_\mu t$$

1. We decided not to add a dark matter candidate

where the first term is the SM lagrangian, and the rest describes the new strongly interacting gauge boson and its interaction with the SM top quark. We make the additional assumption that Z' decays only in $t\bar{t}$.

This kind of model (linked to Randall-Sundrum) tends to suppress couplings to light fermions compared to right-handed top. We consider $g_R^t = 3$, this value is arbitrary in this generic model. Then, the width of Z' is given by :

$$\Gamma = \frac{g^2}{24\pi} \cdot \sqrt{1 - \frac{4m_t^2}{M_{Z'}^2}} \frac{M_{Z'}^2 - 2m_t^2}{M_{Z'}}$$

Finally, the production cross-section for Z' computed using MadGraph4 LO generator is shown in fig. 19.

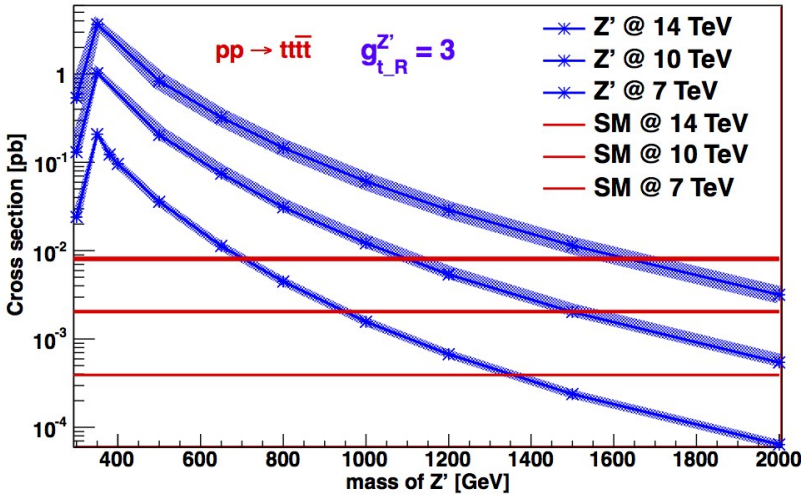

FIGURE 19 – Z' production cross-sections at different c.o.m energies

2.3. Top exotics partners

This model is built around two blocks : the SM sector and the composite one which includes two $SU(2)_L$ doublets as (t_L, b_L) exotic partners, a singlet $\tilde{T}$ for t_R and a Higgs doublet :

$$Q = \begin{bmatrix} T & T_{5/3} \\ B & T_{2/3} \end{bmatrix}, \quad \tilde{T} \quad , \quad H = \begin{bmatrix} \phi_0^* & \phi^+ \\ -\phi^- & \phi_0 \end{bmatrix}$$

The two doublets in Q have respectively a hypercharge of 1/6 and 7/6. So (T, B) has the same quantum numbers as (t_L, b_L), while ($T_{5/3}$, $T_{2/3}$) contains an exotic state with charge 5/3 and a top-like $T_{2/3}$.

Now, writing the full lagrangian :

$$\left.\begin{aligned} L = \bar{q_L}\not{\partial} q_L + \bar{t_R}\not{\partial} t_R \end{aligned}\right\} \quad \text{Elementary sector}$$

$$\left.\begin{aligned} &+ Tr(\bar{Q}(\not{\partial} - M_Q)Q) + \bar{\tilde{T}}(\not{\partial} - M_{\tilde{T}})\tilde{T} \\ &+ Y_* Tr(\bar{Q}H)\tilde{T} + hc \end{aligned}\right\} \quad \text{Composite sector}$$

$$\left.\begin{aligned} + \Delta_L \bar{q_L}(T, B) + \Delta_R \bar{t_R}\tilde{T} + hc \end{aligned}\right\} \quad \text{Mixing}$$

The lagrangian gives mass eigenstates in terms of mixing coefficients :

$$|\text{SM}> = cos\phi \ |\text{Elementary}> + sin\phi \ |\text{Composite}> \ ; \ \text{with} \ \tan\phi_{L/R} = \frac{\Delta_{L/R}}{M_Q}$$

Concerning the $T_{5/3}$, in the eigenstate basis, the relevant part is

$$\frac{g}{\sqrt{2}}(sin(\theta_{T_{2/3},t_R})\bar{T_{5/3}}\gamma^\mu W^+_\mu t_R + sin(\theta_{T_{2/3},t_L})\bar{T_{5/3}}\gamma^\mu W^+_\mu t_L$$

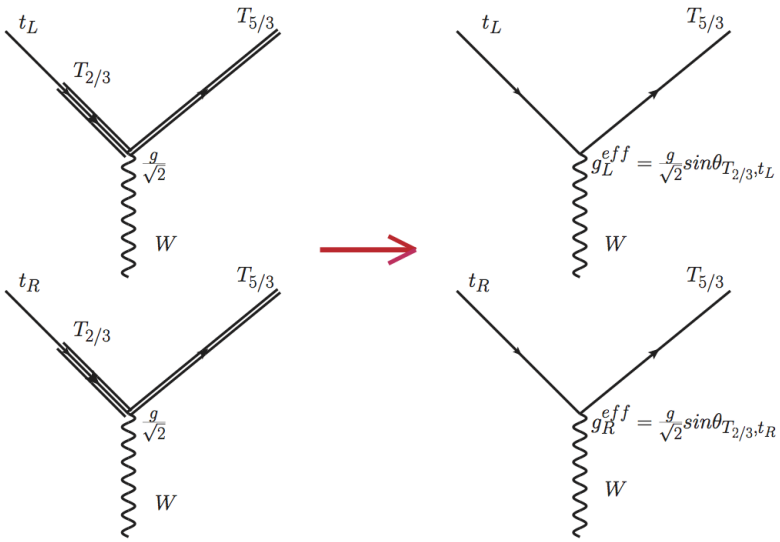

FIGURE 20 – Mixing diagrams and their effective equivalents

As shown in fig. 20, the top couples to $T_{5/3}$ by its $T_{2/3}$ component, but it can be modeled by an effective coupling between the top and its exotic partner. Knowing these rules, we can present the different types of production : the $T_{5/3}$ pair production is done by pure QCD and gives a $t\bar{t}W^+W^-$ final state, similar to $t\bar{t}t\bar{t}$, while the single production is very sensitive to the $T_{5/3}$-tW coupling which parametrizes its cross-section. The corresponding Feynman diagrams are reproduced in fig. 21.

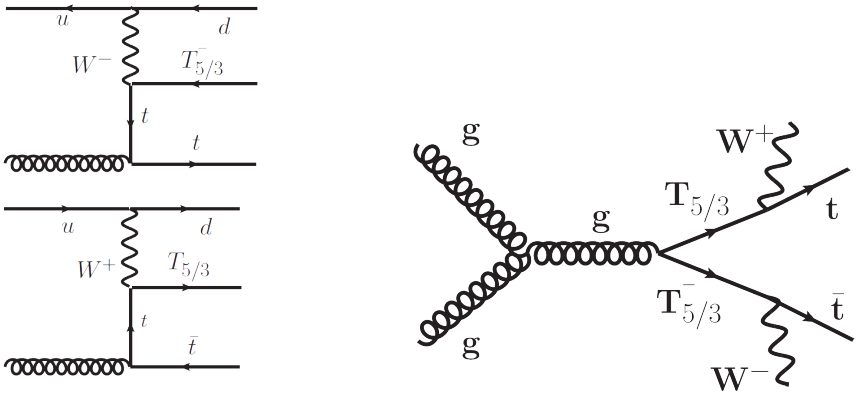

FIGURE 21 – $T_{5/3}$ single and pair production

The width is then computed from the lagrangian, depending on the $T_{5/3}$ mass M and the coupling λ ($T_{5/3}$-tW) :

$$\Gamma = \frac{\lambda^2 M}{32\pi}((1+\frac{m_t^2 - m_W^2}{M^2})(1+\frac{m_t^2 + 2m_W^2}{M^2})-4\frac{m_t^2}{M^2})\times\sqrt{1-2\frac{m_t^2+m_W^2}{M^2}+\frac{(m_t^2-m_W^2)^2}{M^4}}$$

where $$\lambda = \frac{g}{\sqrt{2}}(\frac{M}{m_W})\sqrt{sin^2(\theta_{T_{2/3},t_L}) + sin^2(\theta_{T_{2/3},t_R})}$$

Thus, the different cross-sections for the $T_{5/3}$ single and pair productions simulated with MadGraph4 are shown in fig. 22.

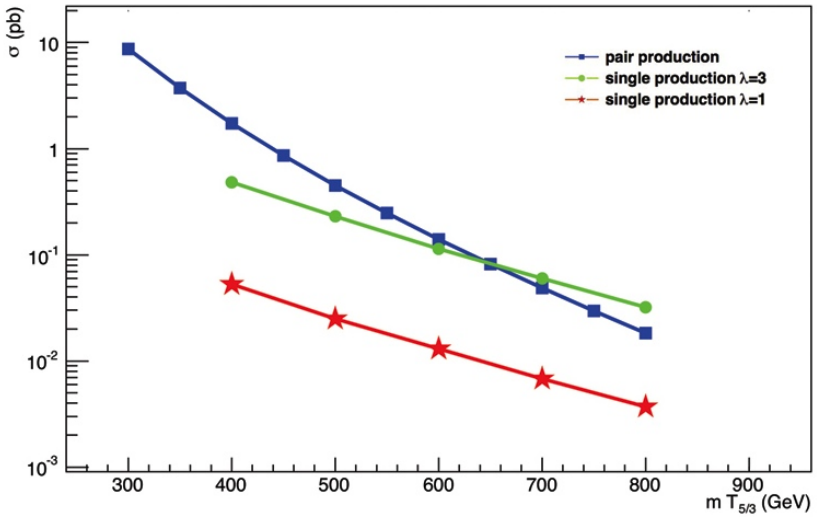

FIGURE 22 – $T_{5/3}$ production cross-sections for different masses at $\sqrt{s}$=8 TeV

2.4. Same-sign dilepton channel

For both models, we have only one decay channel : $Z' \to t\bar{t}$ and $T_{5/3} \to tW^+$. We know that the top quark decays only in $t \to bW^+$ (99,9%). Then, the different decays of the W boson are either hadronic ($u\bar{d}, u\bar{s}, u\bar{b}, c\bar{d}, c\bar{s}, c\bar{b} = 67{,}6\%$) either leptonic ($e^+\nu_e, \mu^+\nu_\mu, \tau^+\nu_\tau$=32,4%). Here we focus only on e and μ decays.

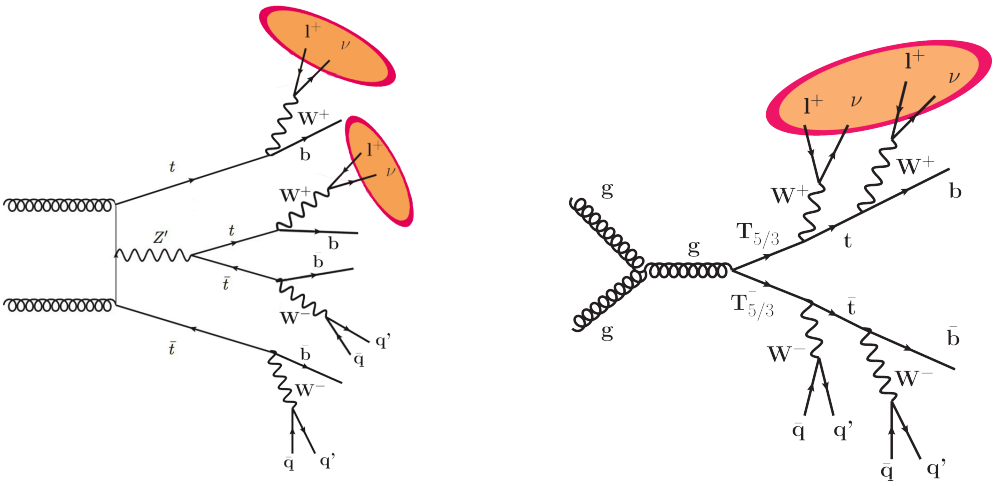

FIGURE 23 – Same-sign signature for both Z' and $T_{5/3}$ searches

The huge interest of this same-sign channel is that it suppresses the main background $t\bar{t}$ which can only form such a leptonic pair very rarely. Indeed, the second lepton can come out from the B mesons shower before passing all the cuts, this is called a *fake* event (fig. 23). What occurs also is a wrong experimental reconstruction of the lepton's charge, thus giving same-sign leptons from the W bosons, this is a *mis-ID* event (fig. 24).

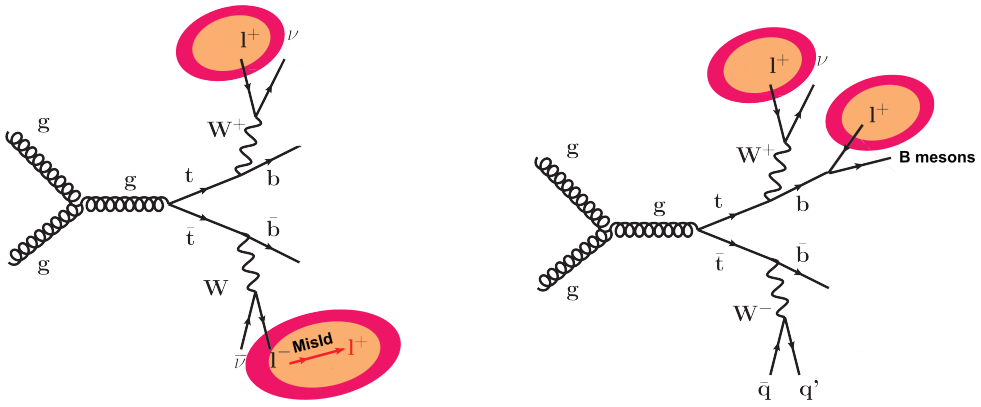

FIGURE 24 – Mis-ID events and fakes

Additionally, for the $T_{5/3}$ pair production, in this channel one can reconstruct the exotic particle's mass using the hadronic branch.

3. Z' discovery potential of the same-sign dilepton channel

I present here the same-sign dilepton analysis for a Z' of 1 TeV in the perspective of enlarging the study to the three leptons channel.

3.1. Samples and methodology

The MC signal samples were produced using MadGraph4 [12], then the final states were obtained using the DECAY tool. The hadronisation (ISR/FSR) was done under Pythia6.4 [26]. The resulting samples were in LHE format and read in Mathematica for the analysis. I first tried to generate $t\bar{t} + 0, 1, 2, 3$ jets background with MadGraph4 but it was beyond the power of the code, so they were produced with MadGraph5 [13] then decayed and hadronised like the signal. The jet clustering was done with a cone algorithm (GETJET) using a clustering radius of 0.4 and a cut on p_T at 30 GeV.

I also included $pp \to (Z') \to t\bar{t}t\bar{t}+1$ jet to increase the statistics. I only focused on $t\bar{t}$ backgrounds [2]. The cross-sections found by MadGraph are reported in Table 2.

Process	σ [fb]	$\sigma.BR(2lSS)$ [fb]
Signal Z'(1TeV)	61	2.6
Signal Z'(1TeV) + 1 jet	21.5	0.9
$t\bar{t}t\bar{t}$	7.5	0.3
$t\bar{t}W^+W^- + 0, 1, 2$ jets	450	13.7
$t\bar{t}W + 0, 1, 2, 3$ jets	595	18.4
$W^+W^-W + 0, 1, 2$ jets	603	18.7
$WW + 0, 1, 2, 3$ jets	340	15.5
$t\bar{t}$	466 000	210
$t\bar{t} + 1$ jet	380 000	170
$t\bar{t} + 2$ jets	211 000	97
$t\bar{t} + 3$ jets	93 000	43
$t\bar{t} + 4$ jets	33 000	15

TABLE 2 – Signal and background production cross-sections (LO)

The reduction from hundreds of picobarns to hundreds of femtobarns is due to a tiny charge misindentification rate. Indeed, if we only select same-sign dilepton pairs, with MG samples we should simply have no background as the

2. I still include $t\bar{t}W^+W^-$ and $t\bar{t}W$ ("other") and $t\bar{t}t\bar{t}$ ("4top from SM") in my plots.

MC generator does not include misidentification of the charge or reconstruction of the fake leptons from the b hadronisation [3]. In order to solve this, we consider that the probability of mis-ID for a muon is 0 and for an electron around 1%. In the facts, this error depends on η and p_T but recent analyses show that 1% is too much overestimated. Thus, the branching ratio for $t\bar{t}$ in the SS dilepton channel is :

$$BR(2lSS) = 4 \times (21.4\%)^2 \times 1\% = 1,8 \times 10^{-3}$$

For the signal, we can compute the branching ratio for each channel (Table 3).

Channel	Branching ratio
0 lepton	21%
1 lepton	26.3%
2 leptons	12.5%
2 SS leptons	4.4%
3 leptons	2.6%
4 leptons	0.2%

TABLE 3 – Signal branching ratios

Eventually, we would like to use the LHC to see if the production rate of the 4 tops is what the SM predicts or if the deviation we could observe is compatible with the presence of a Z' resonance, and so with a strong sector. One needs to know which mass range can be tested at 14 TeV or, reversely, at which luminosity should we observe (5σ) the Z'(1 TeV). The idea is to filter events and make cuts on parameters so that the background is mostly cut while the signal keeps sufficient events. To do so, we need to plot the different distributions to find cuts. If easy cuts, like H_T, jet or bjet multiplicities, are not efficient enough, one needs to go further, looking at the invariant mass of the leptons, or the p_T of the second lepton, or the distance between jets and leptons. We will work with $\mathcal{L}$=10 fb^{-1}.
The different numbers of generated events for each sample are given in Table 4.

Sample	2l generated	2 hard SS leptons	σ (fb)	σ.BR(2l) (fb)
Signal	16 003	6 007	62	2.8
Signal + j	13 776	5 290	20	0.9
$t\bar{t}$	33 328	11 025	466 000	21 000
$t\bar{t}$ + 1j	33 326	11 389	380 000	17 000
$t\bar{t}$ + 2j	33 323	11 776	211 000	9 700
$t\bar{t}$ + 3j	19 996	7 219	93 000	4 300
$t\bar{t}$ + 4j	3 355	1 251	33 000	1 500

TABLE 4 – Signal branching ratios

3. In this phenomenological study, we did not add detector effects like Geant4

The huge difference between the production rate of the signal (fb) compared to the background (pb) seems to kill any possibility to extract useful information. After the mis-ID factor, the signal/background ratio is around 1%. Now, let us try to reduce it further using cuts. For each event, we have kept only hard jets (p_T $\geq$30 GeV) and every lepton, soft or hard. First, we will have a look at the bjet multiplicity (fig. 25), as it gives a good overlook on our strategy.

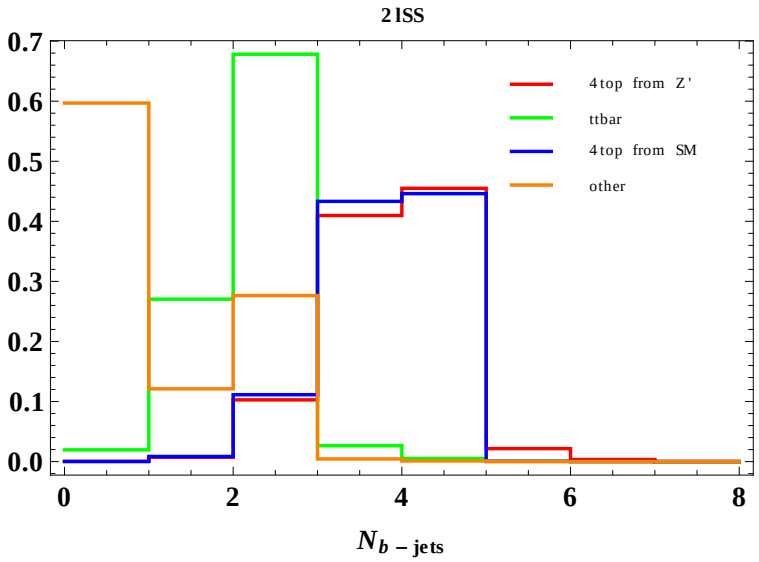

FIGURE 25 – Hard b-jets multiplicity in the SS 2l channel

The first cut we could apply is Nb(b-jet) ≥ 3 which rejects about 95% of the background for 10% of signal. The $\frac{S}{B}$ ratio becomes 20%. Now, for the jet multiplicity in fig. 26, a good cut would be at leat 5 ou 6 jets.

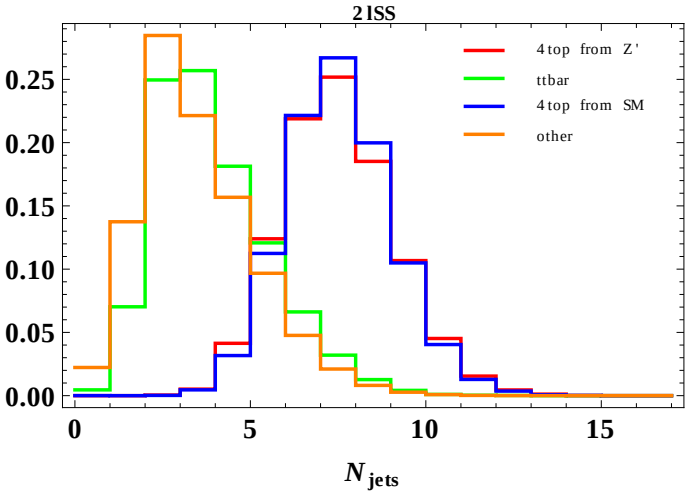

FIGURE 26 – Hard jets multiplicity in the SS 2l channel

H_T, the total transverse momentum, is defined by the sum of the transverse momentum of jets and leptons with $p_T \geq 30$ GeV (fig. 27).

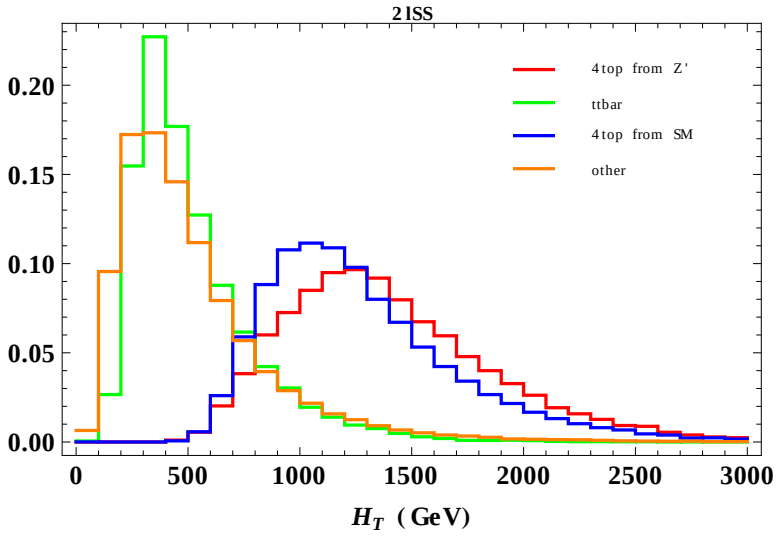

FIGURE 27 – H_T distribution in the SS 2l channel

The logical cut would be between 800 and 1400 GeV. Let us have a look at the H_T and n_{jets} plots for each background in fig. 28. Applying the cuts we found will nearly suppress $t\bar{t}$+0,1j and favour $t\bar{t}$+3,4 j.

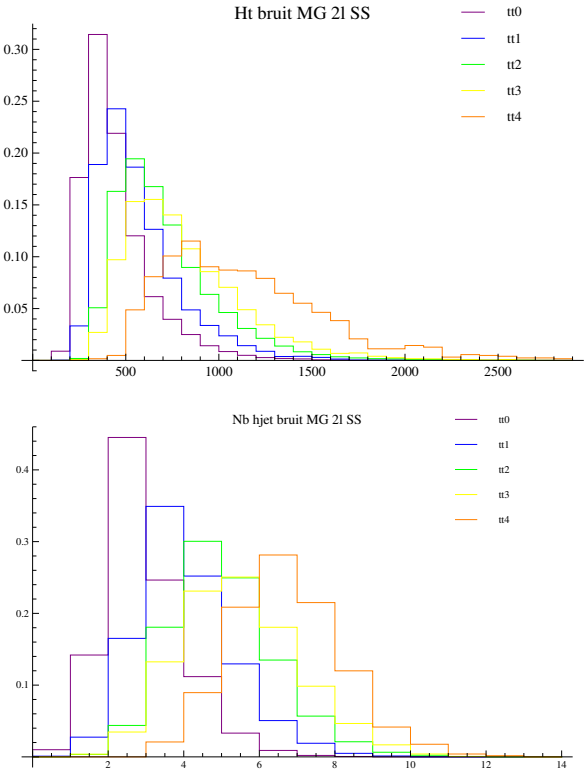

FIGURE 28 – H_T and jet multiplicity for each background

3.2. Cuts

In order to scan the parameter space, we will try several configurations of cuts (C1 to C15) on H_T, jet and bjet multiplicities, in order to find the optimal ones. The core cut is the b-jet one which has a very good efficiency. Once we have applied our cuts, we rescale each number of events to a common luminosity of 10 fb^{-1} to estimate the significance $\sigma = \frac{S}{\sqrt{B+1}}$.

Cut	bjet	jet	H_T	S_{tot}	B_{tot}	σ
C1	2	5	500	33	751	1.2
C2	2	6	500	29	409	1.4
C3	3	6	500	27	56	3.5
C4	3	6	700	26	41	4.1
C5	3	6	800	25	33	4.4
C6	3	6	1000	22	19	5
C7	3	6	1200	17	10	5.5
C8	3	6	1300	15	7	5.4
C9	3	5	1000	25	23	5.2
C10	**3**	**5**	**1200**	**19**	**11**	**5.7**
C11	**3**	**5**	**1300**	**16**	**8**	**5.7**
C12	-	7	600	21	197	1.5
C13	-	7	700	21	174	1.6
C14	-	7	1100	16	67	2
C15	-	8	800	20	143	1.7

TABLE 5 – Number of passing events for different cuts configurations

Cut	S_{tot}	S	S+j	B_{tot}	$t\bar{t}$	$t\bar{t}$+1j	$t\bar{t}$+2j	$t\bar{t}$+3j	$t\bar{t}$+4j	σ
C1	33.1	24.4	8.7	751.4	56.8	202.6	256.2	139.8	96.	1.2
C2	28.8	20.8	8.	409.2	17.6	86.9	138.7	89.8	76.2	1.4
C3	26.6	19.3	7.3	56.4	1.7	10.7	19.4	13.9	10.7	3.5
C4	26.2	18.9	7.3	41.2	1.	7.	13.5	10.2	9.5	4.1
C5	25.3	18.1	7.2	32.9	0.6	5.6	10.2	8.2	8.3	4.4
C6	21.9	15.3	6.6	19.	0.1	2.4	5.8	4.7	6.	5.
C7	17.2	11.7	5.5	9.9	0.1	0.7	2.7	2.2	4.2	5.5
C8	14.6	9.8	4.8	7.2	0.	0.4	1.8	1.5	3.5	5.4
C9	24.6	17.5	7.1	22.6	0.1	3.6	7.	5.3	6.6	5.2
C10	**19.2**	**13.3**	**5.9**	**11.2**	**0.1**	**0.9**	**3.1**	**2.5**	**4.6**	**5.7**
C11	**16.3**	**11.1**	**5.2**	**8.1**	**0.**	**0.6**	**2.1**	**1.7**	**3.7**	**5.7**
C12	21.3	14.8	6.5	197.4	4.2	30.6	60.4	48.1	54.1	1.5
C13	21.1	14.6	6.5	173.9	3.3	25.9	51.6	41.9	51.2	1.6
C14	16.1	10.7	5.4	67.4	0.9	7.2	15.7	15.2	28.4	2.
C15	20.4	14.	6.4	143.3	2.3	20.4	40.5	34.5	45.6	1.7

TABLE 6 – Detailed passing number of events for each sample

The numbers in Tables 5 and 6 depend on a lot of parameters during the generation and the sample size, so it may differ slightly with different samples. It gives a good view on which cuts are efficient : C7, C10 and C11.

The best cuts are :

— number of b-jets ≥ 3
— number of jets ≥ 5 or 6
— $H_T \geq 1200$ or 1300

The standard value of $\sigma = 5$ is required to proclame a discovery, so we estimate the discovery luminosity with this formula :

$$\mathcal{L}_{disc} = \frac{5\mathcal{L}}{2S^2}(5B + \sqrt{25B^2 + 4S^2})$$

Thus, the discovery luminosity is about 8,5 fb^{-1} at 14 TeV for a Z' of 1 TeV.

For consistency, if we want to compare this to the extensive study already done, one should add every background as $t\bar{t}$ is only about 88% of the total background in this channel. Eventually, the discovery luminosity should raise a little bit as the significance drops, but globally the optimal cuts are the same.

3.3. Extensions

The previous result corresponds to a specific mass (1 TeV) but also to a specific coupling (g=3). One interesting question could be the dependence of such cuts on the coupling constant and the mass. I will focus on the impact of these parameters on H_T as they do not have any impact on the events topology. As expected, H_T shifts with a different mass (fig. 29). The saturation of the maximum characterizes the effective theory range.

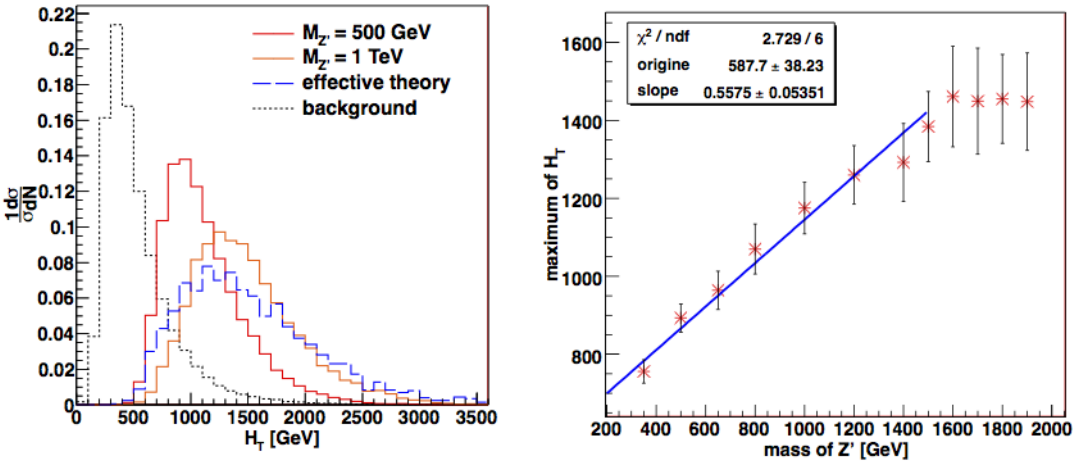

FIGURE 29 – H_T distribution for different Z' masses

But if we change the coupling while keeping the mass unchanged, the Z' width will still change but not H_T. To see a difference, we need to select specifically the top pair coming from the Z' and plot, for instance, their invariant mass (fig. 30) ; we will see the impact of the width, indeed. But H_T does not change, the main reason being that eventually it is impossible to know which top comes from the Z' killing any correlation between its width and global observables.

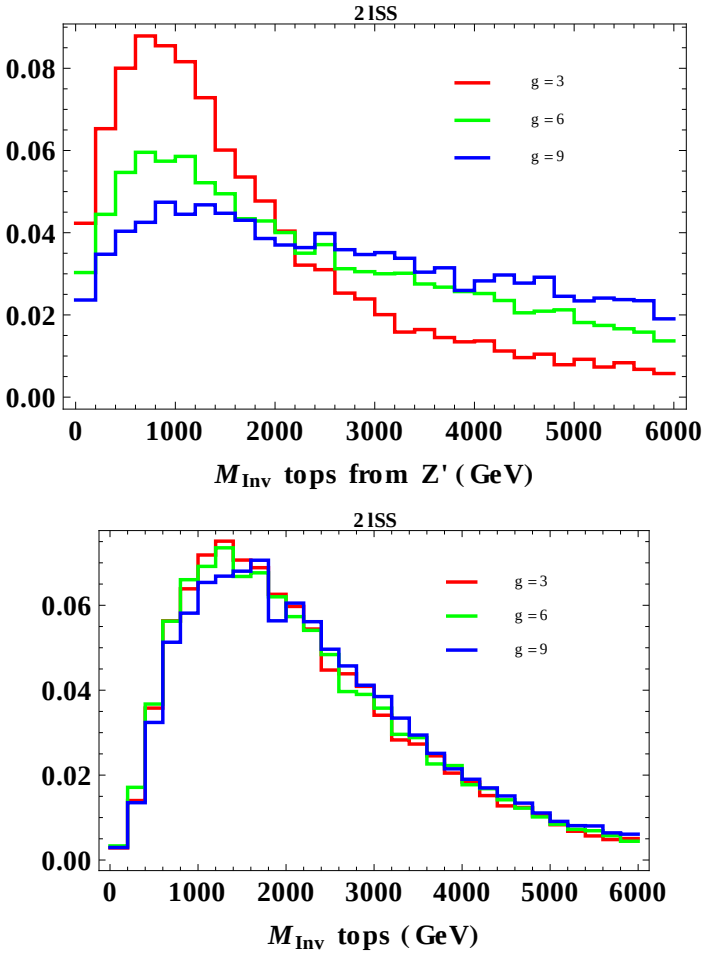

FIGURE 30 – Invariant mass of $t\bar{t}$ pair from Z' and H_T for different widths

In short, the optimized cuts stay unchanged with a different coupling. Using the relation between the maximum of H_T and the Z' mass, one could also reconstruct the mass. Now, we have seen that the same-sign dilepton channel is the golden channel for such analysis, but we can try the trilepton channel to see if it can increase the statistics.

4. Z' discovery potential of the trilepton channel

4.1. Motivation

During my master thesis, I did not study the 1 lepton channel because the former results on this channel were not promising. At $\mathcal{L}$=10 fb^{-1}, there were 126 signal events against 8217 background events, giving a significance of 1.4 and a discovery luminosity of 129 fb^{-1}. In comparison, the SS dilepton channel was really successful. It is legitimate to wonder if going further in the multilepton channels would increase the sensibility to new physics [4]. The trilepton channel seemed compelling for one reason : while the signal amount is just half it was for the SS dilepton, the background should be almost inexistent, as the third lepton would not come from a W (there are only 2) but from a b-jet or an additional jet. The probability that such a lepton would pass a kinematical cut p_T $\geq$30 GeV seemed very little. The goal of my investigation was to quantify the sensibility of the LHC to 4-top production in the trilepton channel.

There is still a technical issue : the MC samples generated by MadGraph4 stand-alone [12] does not include the fake leptons radiated by the B mesons shower. As for now, the $t\bar{t}$ backgrounds would not pass the 3 leptons cut. With the help of Juan Rojo, we implemented an alternative way in order to have these leptons. Once the $t\bar{t}$ samples have been decayed, they are processed by Pythia8 [27] and the outgoing particles are filtered so that the leptons are kept somewhere while all the hadrons are clustered in jets by FastJet [30] using the SISCone plugin [10]. As a result, we obtained a homemade file which includes only jets and leptons. This is the first problem : we do not have b-tagged jets anymore. As we know that the bjet cut was the most crucial in the SS dilepton channel, this is rather worrying. We need to find other efficient cuts or a way to obtain a kind of b-tagging [5].

The second problem is that the channel is now trilepton and no more same-sign dilepton, which means that we do not rely on the small charge misidentification rate any more. We loose the misid factor of 1% which was also very crucial.

As for the MC generation, since the trilepton channel is a very tiny subset, one needs to generate a lot of events in MadGraph. This is because in DECAY, we can only choose to decay family by family, for example, every top quark in W electron + b quark ; or every antitop quark in W jets + bbar quark.

4. Indeed, for SUSY searches with high MET, the trilepton channel is investigated
5. Of course, using Geant4 in Athena would do it but we do not want to use a black box

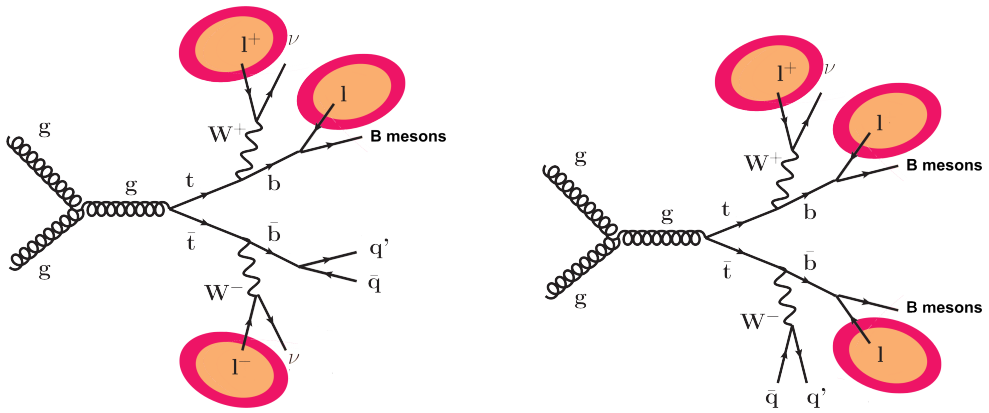

FIGURE 31 – WWb and Wbb events

The three leptons channel for $t\bar{t}$ consists in two sub-events (fig. 31) : those where two leptons come from the W's and only one from the b quark (WWb) and those where this is the opposite situation (Wbb). We naturally expect that Wbb should occur less often than WWb. We verify it in order to focus the MC generation only on WWb (= every $t, \bar{t}$ in leptonic Ws) and reasonably omit the Wbb generation (= every t in leptonic W and every $\bar{t}$ in everything + reverse situation). For this, we used an enormous sample to check the number of remaining trilepton events requiring a cut on p_T, see fig. 32 and 33.

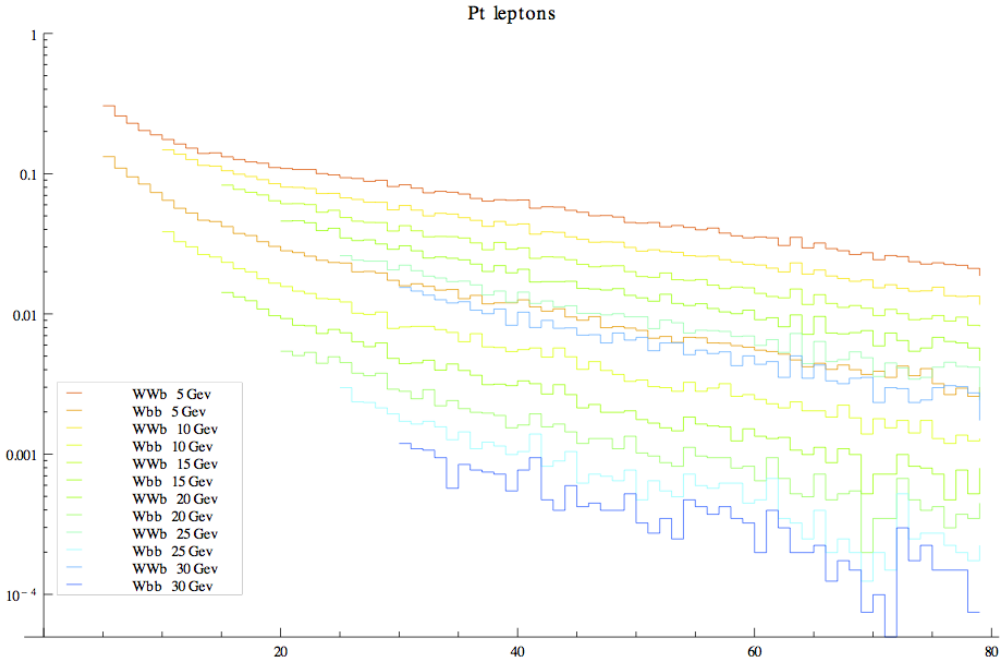

FIGURE 32 – p_T distribution of the leptons for different minimal p_T cuts

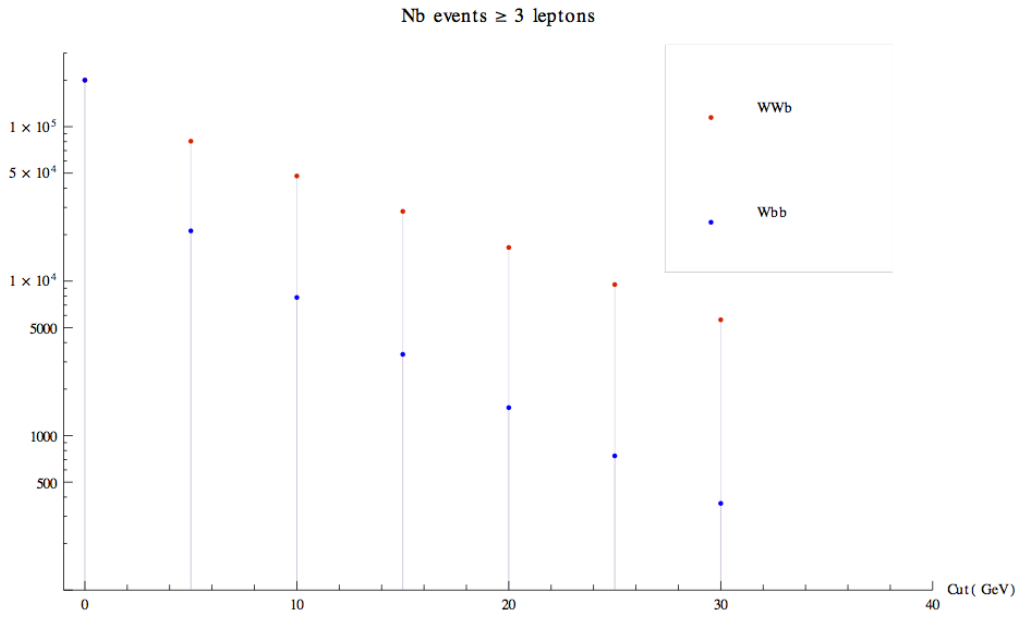

FIGURE 33 – Number of trilepton events for different minimal p_T cuts

4.2. Cuts

If we apply a standard cut at 30 GeV, we see in fig. 33 that the ratio Wbb/WWb is 0,05. It justifies that we focus now only on WWb events. There is an other technical issue linked to the radiations generated by Pythia : there are also soft leptons coming from ISR/FSR in these events so we have to cut at 30 GeV, for example and then select only the trilepton events. Or we can select those which have at least 3 leptons, but due to the branching ratio of the 4 leptons channel, with the 30 GeV cut, it tends to be only trileptons.
The estimated branching ratio for the background, including Wbb, is then :

$$\begin{aligned} BR(\geq 3l) &= 2 \times BR(WWb) + 2 \times BR(Wbb) \\ &= 2 \times (BR^2(W \to l) \times BR(b \to l) + BR(W \to l) \times BR^2(b \to l)) \\ &= 2 \times ((\frac{2}{9})^2 \times BR(b \to l) + \frac{2}{9} \times BR^2(b \to l)) \end{aligned}$$

Using the Particle Data Group tables [28], we can estimate the probability of having a lepton from B mesons to 18%, giving a branching ratio of 3.2%, which is 100 times worse than the dilepton channel. The remaining observables are the jets multiplicity and H_T, which look very similar to the previous channel.

Here are the different cuts we tried :

— Combined cuts on jets multiplicity and H_T : max σ= 0.1

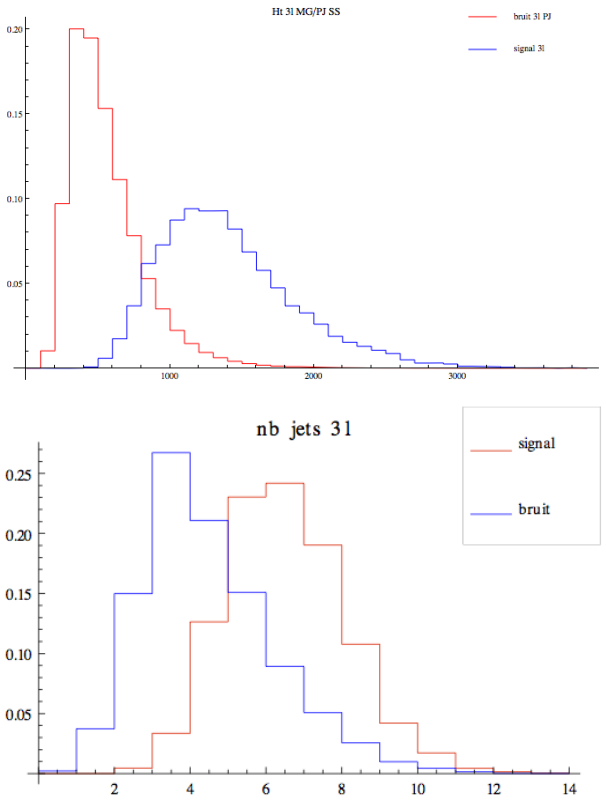

FIGURE 34 – H_T and hard jet multiplicity distributions in the trilepton channel

— Requiring a minimum p_T for the three leptons : max σ= 0.2

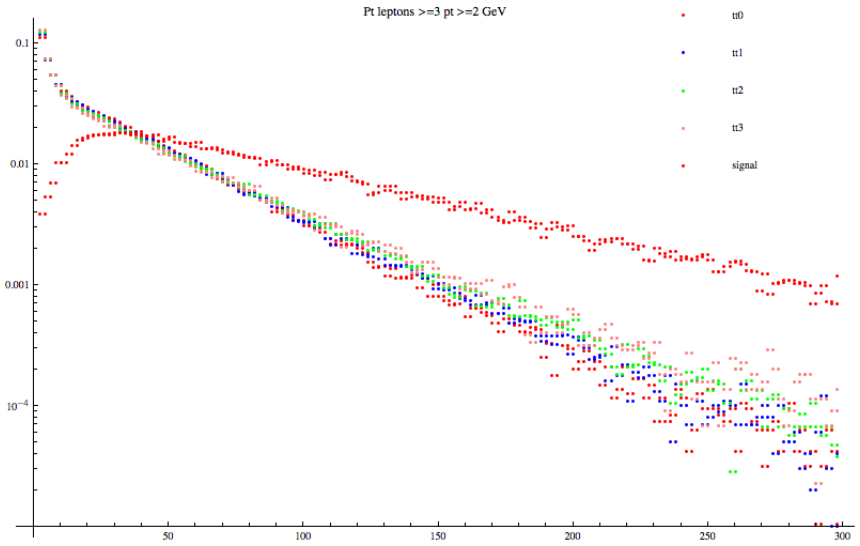

FIGURE 35 – p_T distribution of the leptons in the trilepton channel

— Requiring a minimum p_T on the 3^{rd} most energetic lepton : max σ= 0.3

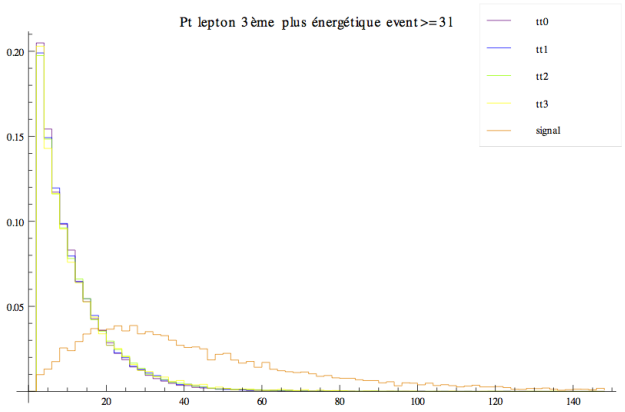

FIGURE 36 – 3^{rd} most energetic lepton p_T distribution

— MET cut : useless

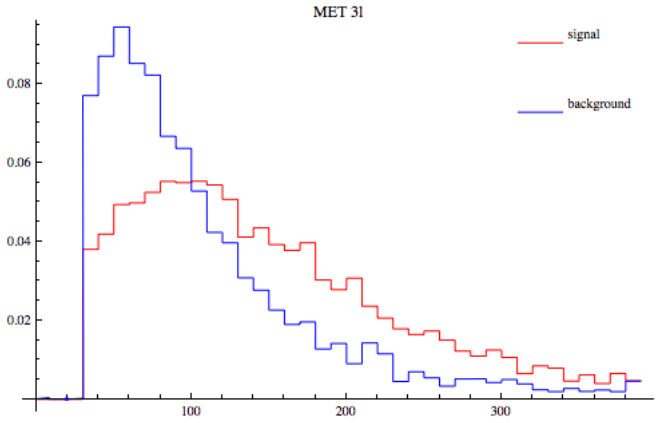

FIGURE 37 – MET distribution

— Using an isolation criteria for the b-jets' leptons : due to the topology of the final state, we did not work out a good criteria.

It is clear that both the b-jet multiplicity and the same-sign criteria are what is missing to make this channel useful compared to the dilepton channel.

In conclusion, with the significance we obtained, in this state, the 3 lepton channel in the absence of b-tagging gives a discovery luminosity around 200 fb^{-1}, which is not conclusive. At the level of this simple "theorist's analysis" in which we do not have any b-tagging algorithm, we cannot do much better, however, it is clear that experimentally, the 3-lepton channel will still be useful after requiring 3 b-jets.It may be best to try to improve the 1 lepton and the dilepton channels with BDT or optimized new criteria.

5. $T_{5/3}$ same-sign dilepton analysis

I present here the exotic study done within ATLAS same-sign dilepton group about $T_{5/3}$. The ultimate goal is to put a limit on its mass using current data - or announce a discovery. It follows the typical structure of any search in ATLAS. We did not have sufficient time to extract a mass limit, it is still under work for a paper for the summer.

5.1. Outline and motivation

Extracting a mass limit from LHC data to constrain a model is what is commonly done for most BSM searches. For this, we generally focus on the predominant production modes to get a result. But here, we make a joint analysis with both pair and single productions : the pair production gives the mass limit while the single production tunes it according to the amount of compositeness due to its sensibility to mixing via the coupling constant.

The current limits with 7 TeV data are given in fig. 38 [18] [6] :

— for low compositeness, $\lambda \ll 1$, expected 624 GeV, observed 677 GeV.
— for normal compositeness, $\lambda \approx 1$, expected 629 GeV, observed 681 GeV.
— for strong compositeness, $\lambda \gg 1$, expected 650 GeV, observed 699 GeV.

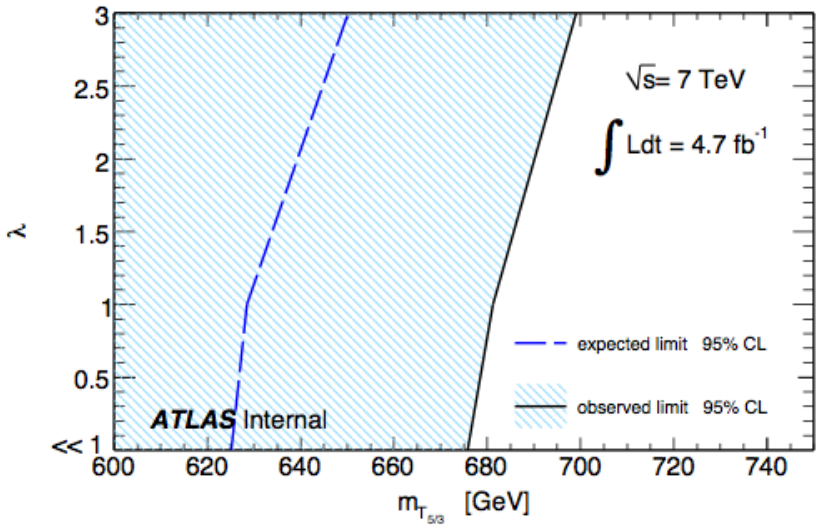

FIGURE 38 – 7 TeV mass limit

6. CMS has released a new limit at 770 GeV for 8 TeV using only pair production

The two heavy fermions $T_{5/3}$ and B behave slightly in the same way, with decay modes $T_{5/3} \to tW^+$ and $B \to tW^-$. The only difference being their charge and consequently the topology of the final state : for the $T_{5/3}$ the same-sign pair is on the same branch, unlike for the B.

Here, the background processes includes three types : the irreducible backgrounds (fig. 39), the mis-ID and the fakes. The irreducible ones are those which have exactly a same-sign dilepton final state, namely *dibosons* (WW, WZ and ZZ), $ttWW$, ttZ and ttW.

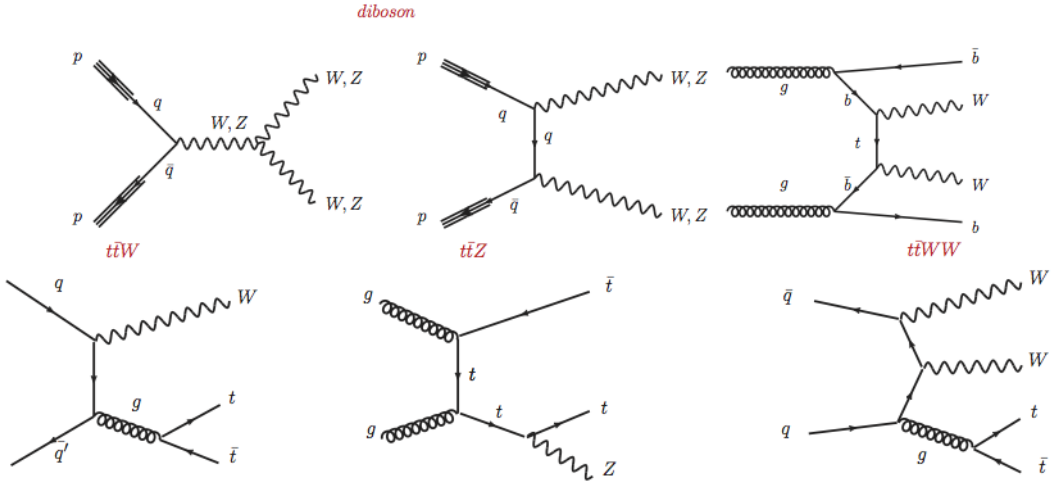

FIGURE 39 – $T_{5/3}$ irreducible backgrounds

The mis-ID will be modeled by a mis-ID factor estimated with a benchmark process ($Z \to e^-e^+$) directly on the data. As for the fakes, their production rate will also be estimated by a matrix method. I had no time to implement these by myself, but for the official 8 TeV search (in winter) I will.

Background	σ	K factor
$t\bar{t}W$	104	1.18
$t\bar{t}W + j$	53.37	1.18
$t\bar{t}W + 2j$	41.48	1.18
$t\bar{t}Z$	67.69	1.34
$t\bar{t}Z + j$	45.35	1.34
$t\bar{t}Z + 2j$	39.77	1.34
WZ	9 750.8	1.06
ZZ	8 734.5	1.11
WW	344.42	1
$tt\bar{W}W$	1.797	1

$m(T_{5/3})$	Pair	λ=3	λ=1
300	8 692	-	-
400	1 732	483	53
500	451	231	25
600	140	114	13
700	49	60	7
800	18	32	4

TABLE 7 – Background and signal cross-sections (fb)

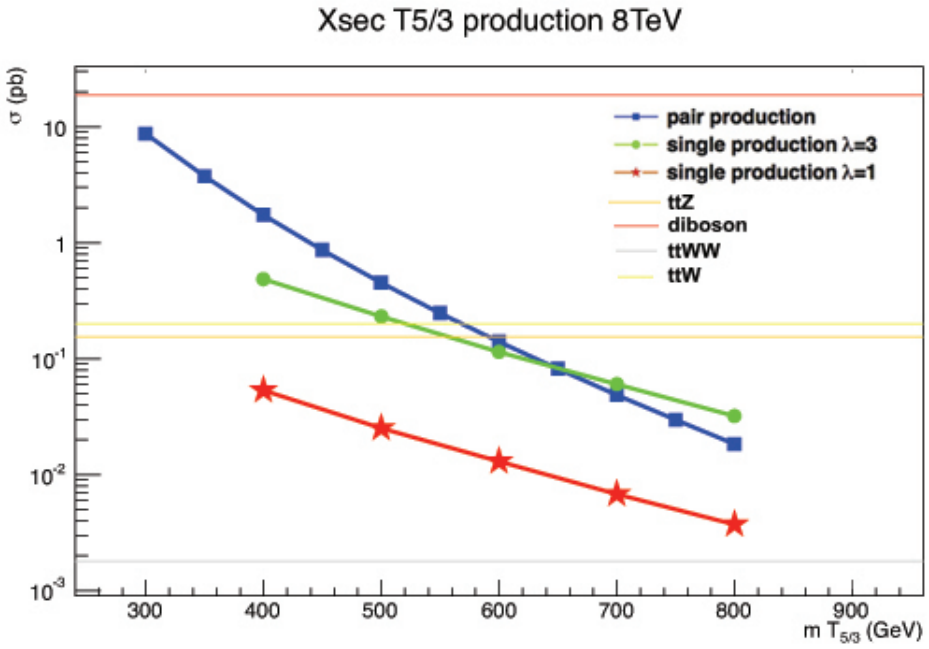

FIGURE 40 – Signal and backgrounds cross-sections at $\sqrt{s}$ =8 TeV

The signal has been generated first using PROTOS [29], a specific top events MC generator, but the model used for the single production based on a mixing matrix between $T_{5/3}$ and the 3 generations was not easy to translate in terms of compositeness degree (embedded in λ). So after a long debating period, we shifted back to MadGraph4 using a model from Roberto Contino [7]. In order to validate the dataset, we needed to generate at least 100k events with a lepton filter ("at least one lepton") for each mass point, then check the kinematic variables to show that everything is okay before submitting it to the ATLAS software for fast simulation or full simulation with Geant4. We made all the validation process for pair production with PROTOS but the move to MadGraph4 occured in May so we did not pass through the software yet.

7. Eventually, we shifted to MadGraph5 due to Pythia8 compatibility issues with the ATLAS software, using VLQ_XTdoubletVL model from M. Buchkremer et ali.

5.2. Cuts in TopRootCore

We apply standard cuts commonly used in every top analysis with some additional criteria. The main observables are listed in fig.41

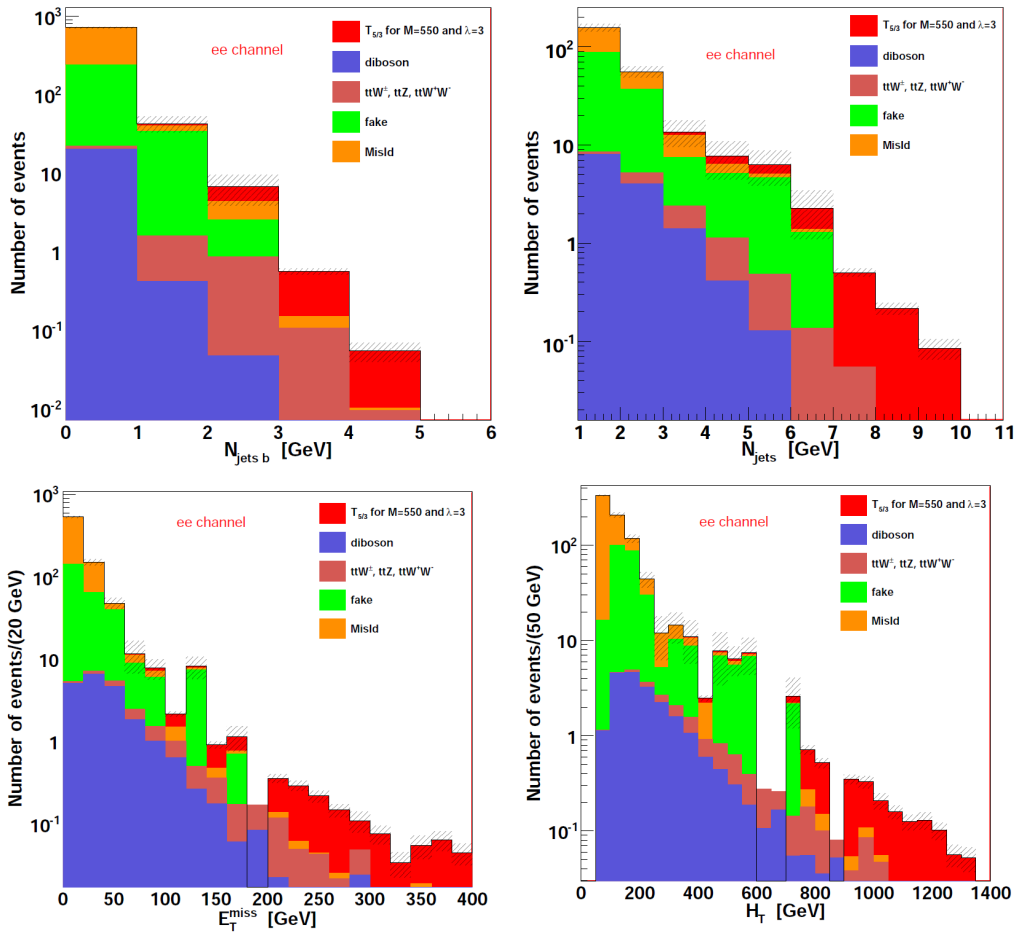

FIGURE 41 – N_{jet}, N_{bjet}, H_T and MET distributions

I will not present the algorithm I wrote using TopRootCore, a generic framework developped for the ATLAS top working group, even though they are what kept me busy debugging for days and weeks.
The common cutflow for same-sign dilepton analyses is the following :

- At least one primary vertex with 5 tracks
- At least one SS lepton pair with channel classification (ee, em, mm)
- Z/quarkonia veto on ee and mm SS pair : the pair invariant mass should be over 15 GeV (quarkonia exclusion) and at least 10 GeV away from the Z peak (91.18 GeV ; Z exclusion)
- At least 2 jets including 1 bjet
- MET$\geq$40 GeV ; H_T $\geq$500 GeV
- For the leptons and jets : p_T $\geq$25 GeV

No optimization have been done as for June on such cuts for $\sqrt{s}$=8 TeV data. As explained before, no $T_{5/3}$ signal have been validated due to the MC generator shift and also some bugs with Pythia using Athena in the last days of the master thesis. A tentative of using B signal instead of $T_{5/3}$ was tried as they both have the same behaviour in pair production :

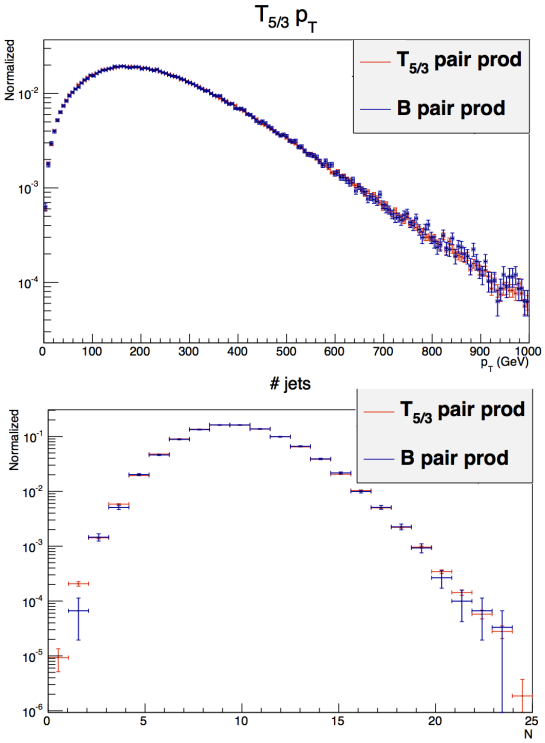

FIGURE 42 – Comparison between $T_{5/3}$ and B distributions

Unfortunately, the analysis using B samples could not be finished before my leaving. The remaining part of this study consists in using matrix methods to estimate the fakes and the misid rate, including the systematics and then extracting a limit using CLs method given the number of events. The *same-sign dilepton* group is planning to release limits on heavy quarks production for summer 2014, in a common exotic VLQ search in same-sign dilepton and trilepton channels.

Conclusions and Outlook

Finally, using MC tools, we found that the same-sign dilepton channel is highly sensitive to a massive resonance which can happen in composite models, with a discovery luminosity of 8.5 fb^{-1} at 14 TeV for a 1 TeV Z'. The trilepton channel would require the implementation of a b-tagging algorithm to properly cut the background which we could not do at the level of our simplified analysis. The $T_{5/3}$ ATLAS analysis is still in progress but combining single and pair productions will definitely improve CMS limit.

For the Z' study, we decided to focus now on the improvement of the same-sign dilepton. The charge mis-ID probability for electrons is actually much smaller than 1%, therefore the dominant background is not coming from charge mis-ID in $t\bar{t}$ events but from faked leptons and rare SM events such as $t\bar{t}W$.

For the $T_{5/3}$ search, we are joining the 8 TeV analysis this fall as the signal is being processed, while preparing the analysis code and checking its consistency with the other groups. A paper combining exotic VLQ searches in the 2lSS and 3l channel is in preparation for the summer conferences.

During this 9 months long master thesis, I have been in contact with two different communities, the theoreticians at CERN and the experimentalists at CEA. This dual experience showed me the real difference between their work and also how they interact together, as the weekly Collider cross-talk at CERN showed me. Each community has its own language and method which eventually should be taken into account to publish results that everyone can exploit. That is why we switched to a model independant $T_{5/3}$ search and used a generic non-ATLAS Z' framework, so that both experimentalists and phenomenologists can reinterpret them.

Time was what I lacked the most. Understanding the theory behind these models, how a MC generator works, how to use the ATLAS software or to submit jobs to the Grid, took a lot of time, even with the great support from other PhD students. Even if I did not succeed to conclude both analysis in 9 months, I am quite satisfied to have understood every step I did.

List of figures

1 SM precision measurements . . . 7
2 SUSY constraints . . . 7
3 Exotic physics constraints . . . 8
4 LHC at CERN . . . 9
5 ATLAS luminosity . . . 10
6 Illustration of the pile-up effect . . . 10
7 Pile-up plots . . . 10
8 Inner structure of the ATLAS detector . . . 11
9 Data processing path in ATLAS . . . 12
10 Example of the grid traffic . . . 13
11 Particle recognition pattern in ATLAS . . . 13
12 Event display including calorimeter and tracking activities . . . 14
13 A representation of the SM . . . 17
14 EWSB sketched by Flip Tanedo on `www.quantumdiaries.org` . . . 18
15 The Standard Model of particle physics in 2013 . . . 18
16 SM four tops events . . . 20
17 Top-philic resonance in $t\bar{t}t\bar{t}$ states . . . 20
18 Resonant production diagrams for Z' . . . 20
19 Z' production cross-sections at different c.o.m energies . . . 21
20 Mixing diagrams and their effective equivalents . . . 22
21 $T_{5/3}$ single and pair production . . . 23
22 $T_{5/3}$ production cross-sections at 8 TeV . . . 23
23 Same-sign signature . . . 24
24 Mis-ID events and fakes . . . 24
25 Hard b-jets multiplicity in the SS 2l channel . . . 27
26 Hard jets multiplicity in the SS 2l channel . . . 27
27 H_T distribution in the SS 2l channel . . . 28
28 H_T and jet multiplicity for each background . . . 28
29 H_T distribution for different Z' masses . . . 30
30 Invariant mass of $t\bar{t}$ pair from Z' and H_T for different widths . . . 31
31 WWb and Wbb events . . . 34
32 p_T distribution of the leptons for different minimal p_T cuts . . . 34
33 Number of trilepton events for different minimal p_T cuts . . . 35
34 H_T and hard jet multiplicity distributions in the trilepton channel 36
35 p_T distribution of the leptons in the trilepton channel . . . 36
36 3^{rd} most energetic lepton p_T distribution . . . 37
37 MET distribution . . . 37

38 7 TeV mass limit 39
39 $T_{5/3}$ irreducible backgrounds 40
40 Signal and backgrounds cross-sections at $\sqrt{s}$ =8 TeV 41
41 N_{jet}, N_{bjet}, H_T and MET distributions 42
42 Comparison between $T_{5/3}$ and B distributions 43

References

[1] ATLAS collaboration, "The ATLAS experiment at the CERN Large Hadron Collider", *JINST 3 S08003*, 2008

[2] CMS collaboration, "CMS Physics TDR", CERN, 2006

[3] Gfitter group, "The Electroweak Fit of the SM after the discovery of a new Higgs Boson at the LHC", arXiv 1209.2716v2, sept 2012

[4] L. Gauthier, "Etudes dans le canal avec deux leptons de même signe de la physique du top au-delà du modèle standard", *CERN-THESIS-2012-157*, 2012

[5] https ://twiki.cern.ch/twiki/bin/view/AtlasPublic/WebHome

[6] ATLAS collaboration, "Evidence for the spin-0 nature of the Higgs boson using ATLAS data", CERN-PH-EP-2013-102, 2013

[7] The CDF and D0 collaborations, "Updated Combination of CDF and D0 Searches for Standard Model Higgs Boson Production with up to 10.0 fb-1 of Data", FERMILAB-CONF-12-318-E, *arXiv :1207.0449*

[8] The ALICE collaboration, "Heavy ion collisions at the LHC ; the ALICE experiment", *hep-ph LIP/96-02*, 1996

[9] The LHCb collaboration, "LHCb : Technical Proposal", *CERN-LHCC-98-004*, 1998

[10] G. Salam and G. Soyez, "A practical Seedless Infrared-Safe Cone jet algorithm", *arXiv :0704.0292*, 2007

[11] G. Salam, M. Cacciari and G. Soyez, "The anti kt jet clustering algorithm", *arXiv :0802.1189*, 2008

[12] MadGraph Collaboration, "MadGraph/MadEvent v4 : the new web generation ", *arXiv :0706.2334*, 2007

[13] J. Alwall, M. Herquet, F. Maltoni and al , "MadGraph 5 : Going beyond", *arXiv :1106.0522*, 2011

[14] R. Contino, "The Higgs as a composite Nambu-Goldstone boson", *arXiv :1005.4269*, 2010

[15] G. Servant and R. Contino, "Discovering the top partners at the LHC using same-sign dilepton final states", *arXiv :0801.1679*, 2008

[16] G. Belanger, A. Pukhov and G. Servant, "Dirac Neutrino Dark Matter", *arXiv :0706.0526*, 2007

[17] G. Servant, L. Gauthier and A.I. Etienvre, "New physics at the LHC : Les Houches report", *arXiv :0802.3715*, 2008

[18] ATLAS collaboration, "Search for exotic same-sign dilepton signatures in 4.7 fb^{-1} of pp collisions at $\sqrt{s}$=7 TeV with the ATLAS detector", *ATLAS-CONF-2012-130*, 2012

[19] ATLAS Collaboration, "Commissioning of the ATLAS high performance b-tagging algorithms in 7 TeV collision data", *ATLAS-CONF-2011-102*, 2011

[20] D. Griffiths, "Introduction to elementary particles", Wiley, 2008

[21] H. Georgi, "Lie algebra in particle physics", 1999

[22] A. Pomarol and J. Serra, "Top quark compositeness, feasibility and implications", *arXiv :0806.3247*, 2008

[23] R. Contino, "A holographic composite Higgs model", *arXiv :0609148*, 2006

[24] A. Wulzer, J. Mrazek, "A strong sector at the LHC : Top partners in same-sign dileptons", *arXiv :0909.3977v2*, 2009

[25] G. Servant, J. Tseng, C. Dennis, M. Karagoz Unel, "Multi W events at LHC from a warped extra dimension with custodial symmetry", *arXiv :0701158*, 2007

[26] T. Sjostrand, S. Mrenna and P. Skands , "PYTHIA 6.4 physics and manual", *arXiv :hep-ph/0603175*, 2006

[27] T. Sjostrand, S. Mrenna and P. Skands , "A brief introduction to PYTHIA 8", *arXiv :0710.3820*, 2007

[28] J. Beringer et al. (Particle Data Group), Phys. Rev. D86, 010001 (2012)

[29] J. A. Aguilar-Saavedra, "Identifying top partners at LHC", *arXiv :0907.3155v2*, 2009

[30] M. Cacciari, G.P. Salam and G. Soyez, "FastJet user manual", *arXiv :1111.6097v1*, 2011

[31] N. Arkani-Hamed, M. Porrati, L. Randall, "Holography and Phenomenology", *arXiv :0012148*

Acknowledgments

I am hugely thankful to both Anne-Isabelle and Géraldine for this great opportunity in exotic physics. It was quite unexpected, just 9 months after having my first course on particle physics, to be at CERN for real. Of course, this leads to another thanks to both KTH professors Jonas and Tommy, whose lectures were the reason why I did this double-degree. I am also very grateful to Bengt for your help for solving an intricate administrative problem between CEA and CERN. I really had a great time with PhD students/post-docs at CERN Theory Division, especially Sercan and Anil for broadening my world to your countries, Rob, Ahmed, Jean-Claude and of course Mateusz. Thanks also Léa for your great help. As for the amazing ATLAS Saclay team, I still have three years to improve my knowledge on zombie movies with you!